Politecnico di Torino

DEPARTMENT OF ELECTRONICS AND TELECOMMUNICATIONS
Master Degree in Electronic Engineering

Master Degree Thesis

Assessing the Impact of an Optical Switch Physical Design in Network Routing Impairments

Supervisors:
Prof. Andrea CARENA
Prof. Paolo BARDELLA
Prof. Vittorio CURRI

Candidate:
Pasquale PASELLA

Academic year 2018-2019

Abstract

Conventional data centers need an efficient interconnection network but electrical switching requires significant power consumption that grows with the data rate and the electrical part became the bottleneck of the transmission.
Today different networks are connected by optical connections that allow to reach high data rates: switching at optical level is convenient
Introduction of optical switching would make an immediate improvement in energy efficiency since it eliminates the O/E/O (Optical/Electrical/Optical) conversions and they could address a larger amount of data increasing the performances.
A candidate technology to sustain these switching devices is Silicon Photonics because it provides small footprint and low power consumption. The main advantage of using this technology is the reduced fabrication cost at large scale.
In this work an optical switch has been designed and analyzed. The starting point was the design of the single elements that composes the switch arriving to characterize it through the evaluation of the BER (Bit Error Rate) of signals that crosses the device under test. The devices were tested by simulation considering a 64-QAM transmission.
This thesis follows the development of the device from physical level, designing the device parameters, up to the system level analysis, where the quality of transmission is evaluated through the bit error rate.

Un ringraziamento ai Professori Andrea Carena e Paolo Bardella per avermi seguito in questi mesi. E' stata una grande opportunità per imparare e soprattutto per crescere.
Un ringraziamento speciale va a Mamma e Papà per avermi dato sempre fiducia durante questo lungo percorso. Hanno reso possibile tutto questo, quindi Grazie.
Ultima ma non per importanza, un grazie alla mia Principessa che mi è sempre vicina in ogni momento. Sei riuscita a rendere tutto più bello e semplice.

Alle tre persone che
mi sono state più vicine
durante questo percorso:
Papà, Mamma e Silvia.
Grazie di tutto.

Contents

1 Introduction **1**
- 1.1 Optical Networks . . . 1
- 1.2 Link . . . 2
  - 1.2.1 Transmitter and Receiver . . . 3
  - 1.2.2 OptSim . . . 7
- 1.3 Benes Switch . . . 8
- 1.4 Ring resonator . . . 9

2 Analysis of RING FILTERS **11**
- 2.1 Physical Parameters . . . 13
  - 2.1.1 Ring of the first order . . . 13
  - 2.1.2 Ring of the second order . . . 14
- 2.2 Voltage selection . . . 15
- 2.3 Ring representation on OptSim . . . 17

3 Analysis of a Benes Switch **20**
- 3.1 Examples of Benes Switch . . . 20
- 3.2 Benes switch in this thesis . . . 22
  - 3.2.1 Benes: Matlab . . . 28
  - 3.2.2 Benes: OptSim . . . 29

4 Analysis of the impact of Benes Switch on a system performance **34**
- 4.1 Characterization of Micro-Rings filters . . . 34
- 4.2 Characterization of the Double Micro-Ring . . . 36
- 4.3 Characterization of the Benes Switch . . . 39
- 4.4 Evaluation of the impact on system performance. . . . 43
  - 4.4.1 Frequency Shift . . . 43
  - 4.4.2 Filter/Power Normalization . . . 44
  - 4.4.3 Simulation Framework . . . 44
  - 4.4.4 Description of the simulation campaign . . . 48

5 Simulation Results **59**
- 5.1 Results: Second Order Ring . . . 59
- 5.2 Results: First Order Ring . . . 64

6 Conclusions **68**

List of Figures

1.1 Attenuation in optical fiber in function of the wavelength. 1
1.2 Elements of an Optical Network. 2
1.3 General scheme of a Transceiver. 3
1.4 Polarization of the electric field in the fiber. 3
1.5 General scheme of transmitter. 4
1.6 Nyquist-shaped spectrum transmitted over the system. . 5
1.7 Constellation of the 64-QAM signal transmitter. 5
1.8 Working band. 6
1.9 General scheme of a coherent receiver. 6
1.10 Block diagram of the transmitter simulated on OptSim. . 8
1.11 Block diagram of the receiver simulated on OptSim. . . . 8
1.12 Logic scheme of a Benes switch. 9
1.13 Scheme of a ring resonator. 10

2.1 Left: Add-Drop configuration. Right: All-Pass configuration. 11
2.2 Scheme of the Double Ring. 12
2.3 Frequency response of the ring normalized with the previously calculated parameters. 14
2.4 Coupling coefficients order in the Double Ring. 15
2.5 Left: Cross state. Right: Bar state. 16
2.6 Frequency response of the ring changing the heating voltage from 7 V to 9 V. 16
2.7 Block scheme of the ring simulated on the software OptSim. 17
2.8 Block diagram used to simulate the single ring. 18
2.9 Mask for fabrication of micro-ring. 18
2.10 Bloch scheme of the second order Ring simulated on OptSim. 19

3.1 Example of Benes structure[1]. 20
3.2 Example of Benes structure[2]. 21
3.3 Second order micro-ring[]. 21
3.4 Benes switch with the corresponding matrices. 22
3.5 One column of the Benes composed by two micro-rings. . 23
3.6 Cross-Cross configuration. 24
3.7 Cross-Bar configuration. 25
3.8 Bar-Cross configuration. 26

3.9 Bar-Bar configuration. 27
3.10 Part of the table obtained from the function "Perm func". 29
3.11 Block scheme of the Benes switch used for the simulations. 30
3.12 Mask fabrication of the Benes switch used. 30
3.13 OptSim scheme of the Benes using the Second order Micro-Ring. 31
3.14 Blocks used to study the Benes. 31
3.15 Frequency response of the Benes with all voltage equal to 0V. 32
3.16 Blocks used to simulated the entire system. 33

4.1 Frequency response of the ring of the Drop Port. 35
4.2 Comparison between Cross state and Bar state in the Drop Port. 35
4.3 Comparison between Cross state and Bar state in the Through Port. 36
4.4 Frequency response of the Drop Port of the Double Ring. 37
4.5 Frequency response of both ports of the Double Ring. . . 38
4.6 Matrix of frequency responses of the Benes Switch with all voltage equal to 0 V. 39
4.7 Frequency response of the Benes with all voltage equal to 0V. 40
4.8 Comparison of $H(F)$ of the Output ports of Benes Switch with V=0 V and V=8.4 V. 41
4.9 Comparison of Benes Switch output between V=0V and V=8.4V. 42
4.10 Raised Cosine transmitted at 32 GBaud at one of the working channel 43
4.11 Raised Cosine transmitted at 64 GBaud at one of the working channel. 44
4.12 Definitions of symbols on OptSim. 45
4.13 Definition of the new name of the variables in the text editor. 46
4.14 Subtitution of the variable name of the previous step with the wanted values. 46
4.15 Command used to launch the OptSim execution. 47
4.16 Code used to calculate the Bit Error Rate for each workspace. 47
4.17 Assignment of the values for each iteration. 48
4.18 OptSim screenshot with one Transmitter and a coherent Receiver. 49
4.19 Comparison between the input signal and the output signal (second order Ring): Case 1. 50
4.20 Comparison between the input signal and the output signal (first order Ring): Case 1. 51
4.21 Comparison between the input signal and the output signal (second order Benes): Case 3. 52

4.22 Comparison between the input signal and the output signal (first order Benes): Case 3. 52
4.23 Input signals generated from 4 Transmitters centered at the four working channels. 53
4.24 Input signals generated from 4 Transmitters centered at the four working channels. 54
4.25 Subplot 2x2 of the output of the Benes with the first order Rings: Case 1. 55
4.26 Subplot 2x2 of the output of the Benes with the second order Rings: Case 1. 56
4.27 Subplot 2x2 of the output of the Benes with the first order Rings: Case 7. 57
4.28 Subplot 2x2 of the output of the Benes with the second order Rings: Case 7. 57

5.1 Table of the best cases. 60
5.2 Subplot 3x2 of the BER with sequences 1234, 1243, 1324, 1342, 1423, 1432. 61
5.3 Subplot 3x2 of the BER with sequences 2134, 2143, 2314, 2341, 2413, 2431. 61
5.4 Subplot 3x2 of the BER with sequences 3124, 3142, 3214, 3241, 3412, 3421. 62
5.5 Subplot 3x2 of the BER with sequences 4123, 4132, 4213, 4231, 4312, 4321. 62
5.6 Penalty of the four ports in the 24 best cases. 63
5.7 Subplot 3x2 of the BER with sequences 1234, 1243, 1324, 1342, 1423, 1432. 64
5.8 Subplot 3x2 of the BER with sequences 2134, 2143, 2314, 2341, 2413, 2431. 65
5.9 Subplot 3x2 of the BER with sequences 3124, 3142, 3214, 3241, 3412, 3421. 65
5.10 Subplot 3x2 of the BER with sequences 4123, 4132, 4213, 4231, 4312, 4321. 66
5.11 Penalty of the four ports in the 24 best cases. 67

1 Introduction

1.1 | Optical Networks

An optical network is a communication net used for the exchange of information through an optical fiber cable. Today the vast majority of all communication on the planet goes through a worldwide network of interconnected optical fibers forming the backbone of the optical network. Among all types of physical links, optical connection is characterized by the lowest attenuation, therefore being the best choice for long distances. In figure 1.1 the attenuation with respect to the wavelength is shown:

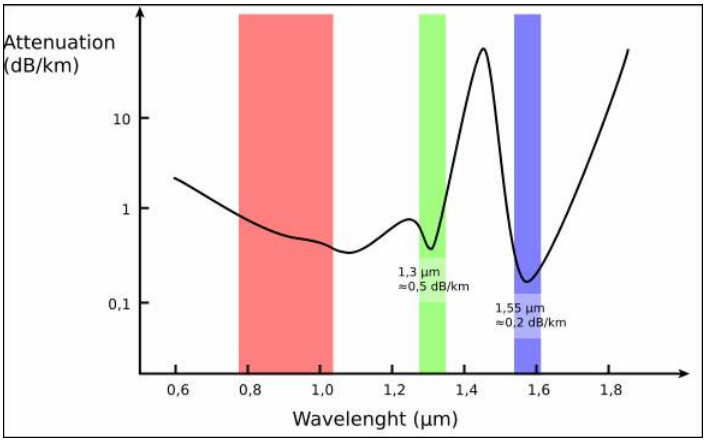

Figure 1.1: Attenuation in optical fiber in function of the wavelength.

The most used band is around 1550 nm (191 THz-196 THz) because the attenuation in this range is lower than 0.2 dB/km. Anyway, even if there is a very low attenuation, the power cannot be increased too much to reach large distances because of non linear effects. The most dominant is the Kerr effect: it is a non linear effect that causes a variation on the glass refractive index as a function of the input power. The variation of the refractive index produces a shift in phase. The higher the input power, the higher the refractive index variation is, therefore when very long distances are involved, the transmitted signal must be periodically amplified.

A typical optical network is composed of the following elements:

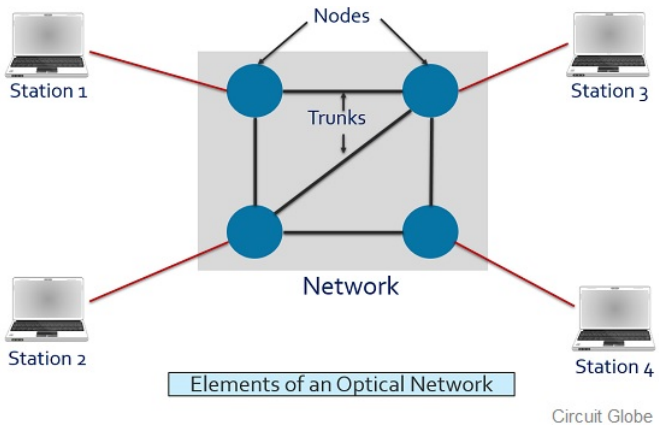

Figure 1.2: Elements of an Optical Network.

There are the stations, the source and the destination of the information connected by optical fibers; between two station there can be nodes in case of multiple transmission lines.
There can be different categories of Optical Networks depending on the area that they connect and the use of the Network.
They are classified as:

- **Local Area Network(LAN):** All users connected are present in a localized area like a building, a department or an office.
- **Campus Network:** It connects multiple LANs.
- **Metropolitan Area Network(MAN):** It permits to connect several buildings present in different cities. Due to its extension, it can be governed by different organizations.
- **Wide Area Network(WAN):** It is employed to establish communication over a large geographical distance and it is controlled and maintained by some private organizations or telecommunication service providers.

1.2 | Link

The general scheme of a communication system is shown in figure 1.3; it is composed by the transmitter (TX), the communication channel and the receiver (RX).

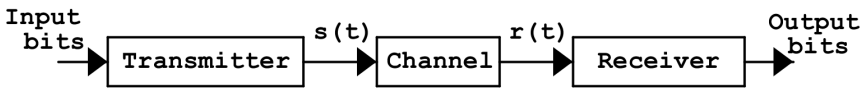

Figure 1.3: General scheme of a Transceiver.

In input there is a sequence of bits that the TX modulates into an analog signal $s(t)$. Once it passed through the communication channel, an additive noise $n(t)$ is added to the original analog signal. The signal in input to the receiver is:

$$r(t) = s(t) + n(t) \tag{1.2.1}$$

1.2.1 | Transmitter and Receiver

The information is transmitted in the fiber thanks to an electro-magnetic field as:

$$E(t) = A(t) \cdot e^{j\phi(t)} \cdot e^{jw_0 t} \tag{1.2.2}$$

that can be expressed as:

$$E(t) = E_R(t) + j \cdot E_I(t) \tag{1.2.3}$$

The fiber carries two independent electrical fields that travel onto orthogonal polarizations, so the light in the fiber is:

$$E(t) = [E_{Rx} + jE_{Ix}]\widehat{x} + [E_{Ry} + jE_{Iy}]\widehat{y} \tag{1.2.4}$$

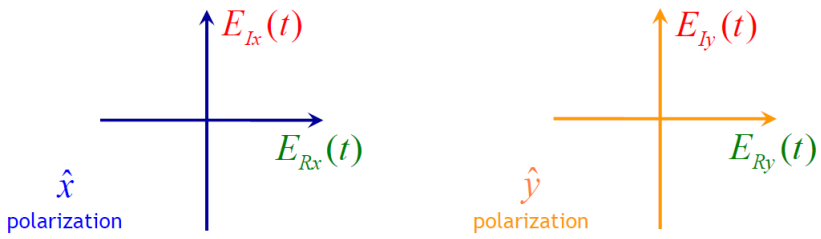

Figure 1.4: Polarization of the electric field in the fiber.

Having the two polarizations, there are four degrees of freedom that can be used with a Phase Modulation-M Quadrature Amlitude Modulation (PM-MQAM) signal. The modulator structure at the transmitter side is shown in figure 1.5.

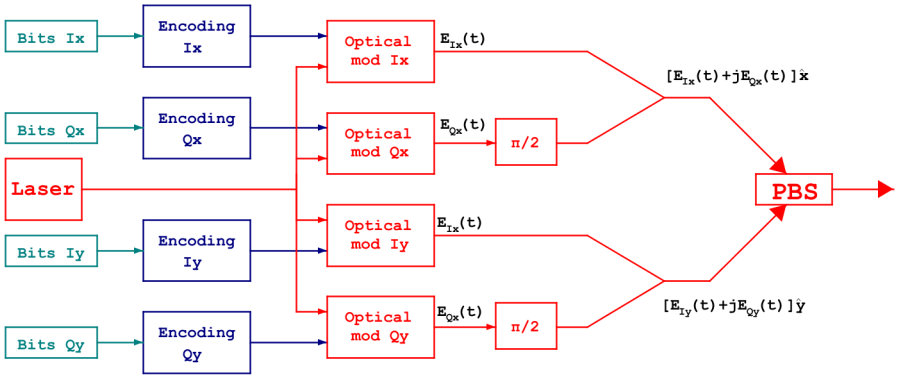

Figure 1.5: General scheme of transmitter.

PBS stands for Polarizing Beam Splitter and it divides the components in the two polarizations. For each polarization, the I and Q components are modulated with an optical source (laser) centered at the carrier frequency and one MZM modulator for each component. The MZM has in input an electrical signal, that contains the information, and the optical source coming from the laser.
The two Q components are shifted by 90^o before being summed in order to construct the constellation.

In this thesis, a PM-64-QAM modulation at 64 GBaud gross symbol rate R_s has been considered with 600 Gbit/s that becomes 768 Gbit/s. This allows to send 6 bits for each "pulse" in the x-polarization and 6 bits for each "pulse" in the y-polarization with a total 12 bits for each pulse. The output spectrum is properly Nyquist-shaped with a roll-off $\rho = 0.2$ and it is shown in figure 1.6.

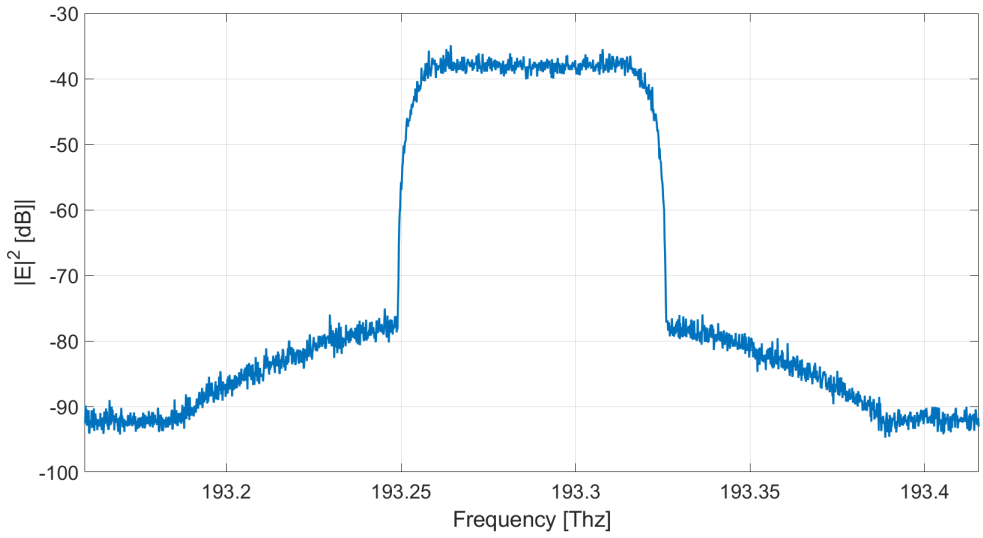

Figure 1.6: Nyquist-shaped spectrum transmitted over the system.

The constellation of the two polarizations built in this modulation is shown in figure 1.7.

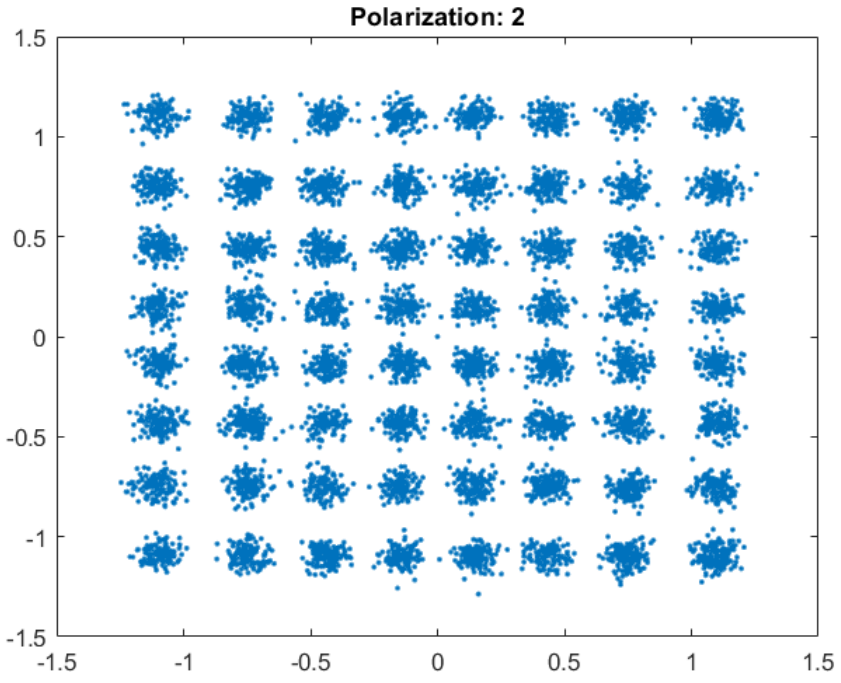

Figure 1.7: Constellation of the 64-QAM signal transmitter.

The channel frequency plan is shown in figure 1.8:

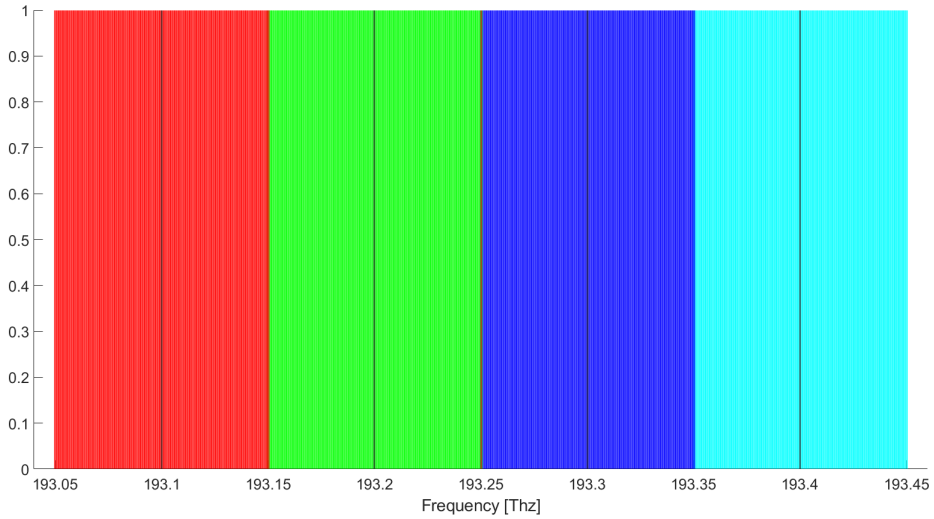

Figure 1.8: Working band.

The band is divided in four channels spaced 100GHz from each other, in order not to have overlapping between two of them. In each of this four channels the Nyquist-shaped spectrum described above is transmitted. The four central frequencies are:

- $f_1 = 193.40THz$
- $f_2 = 193.30THz$
- $f_3 = 193.20THz$
- $f_4 = 193.10THz$

To demodulate complex signals at the receiver side, coherent receivers are used. The block diagram of a general coherent receiver is shown in figure 1.9.

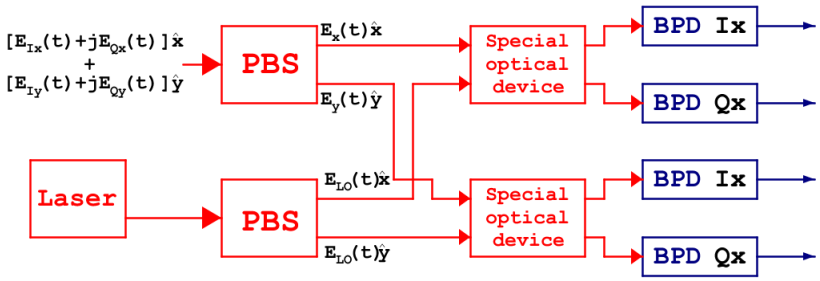

Figure 1.9: General scheme of a coherent receiver.

BPD means Balanced Photo Detector and it is the transition element between optical and electrical regime.
The transmitted signal interferes inside an optical hybrid with a LO-signal provided by another CW-laser converting both quadratures of X- and Y-polarization into the electrical domain.
The receiver always extracts four orthogonal components, however there is the possibility that they are not aligned with those of the transmitter. Through electrical DSP it is possible to "re-align" the reference axes to the transmitted ones and decode the signal correctly.

1.2.2 | OptSim

The software used to simulate the components is OptSim. OptSim is a software tool for the design and simulation of optical communication systems at the signal propagation level. It belongs to the Optical Part of the Company Synopsys. It has a easy-to-use graphical user interface with a large variety of blocks and components that can be found in the library.
An additional software used in this work is OptoDesigner; it covers the physical part of a project. The component simulated on OptSim can be directly reported on OptoDesigner in order to see and modify the mask. There is a direct integration between the programs and this allows to analyze rapidly the behaviour of a device and immediately have an idea for example of the physical occupation.
In this work, in addition to the Benes, also the transmitters and the receivers are reported on OptSim.

The block diagram of the transmitter is displayed in figure 1.10.

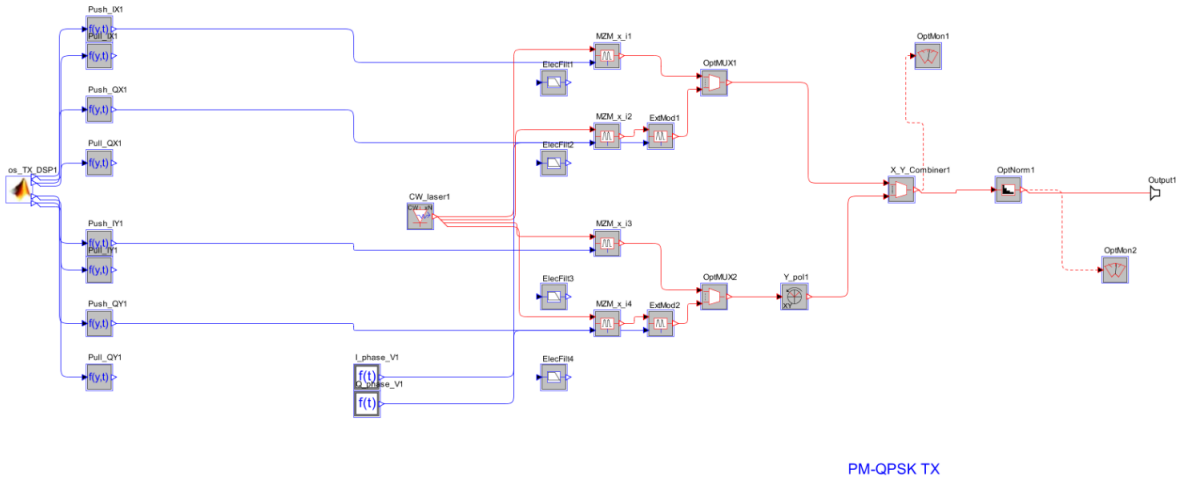

Figure 1.10: Block diagram of the transmitter simulated on OptSim.

The block diagram follows the idea of the transmitter shown in figure 1.5; in this case the symbols generation is implemented with MATLAB.

Regarding the Receiver, the block diagram used for this work is displayed in figure 1.11:

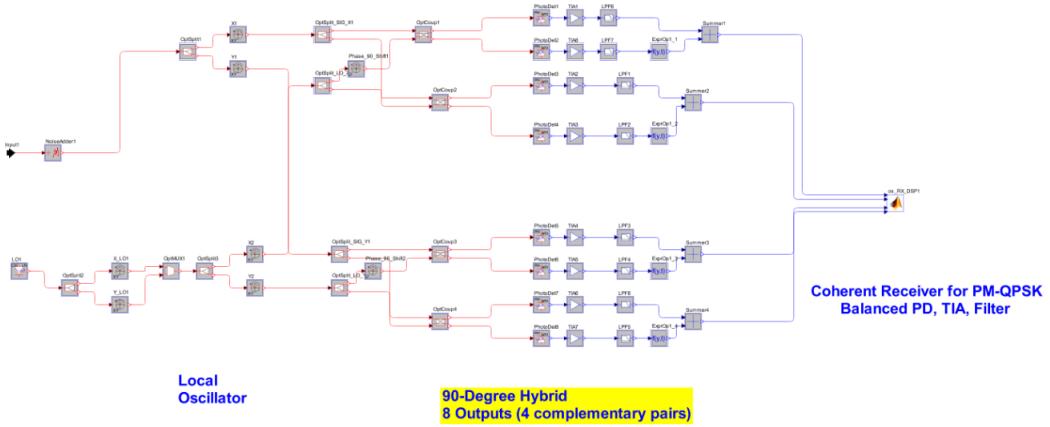

Figure 1.11: Block diagram of the receiver simulated on OptSim.

The electrical DSP, as the trasmitter, is simulated with MATLAB.

1.3 | Benes Switch

As described above, an optical net is composed by different nodes. To each node arrives an optical fiber with many resonant lambda using the Wavelength Division Multiplexing (WDM). All this lambda are then divided with a WDM demultiplexer and finally each lambda reaches the

re-configurable switch fabric. This device can be composed by many Benes structures, each one with the structure designed and simulated in this thesis.
Until today, significant progress has been made with various high performance devices including modulators, photo-detector, switches.
In this thesis the behavior of an optical switch 4x4 has been studied known as Benes switch.
The aim of this component is to direct one of the inputs to a specific output port changing properly six voltages in input.
The general scheme of the Benes is shown in figure 1.12.

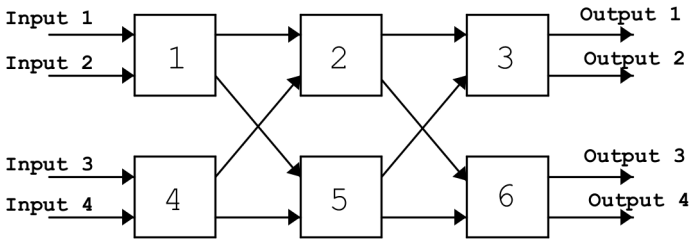

Figure 1.12: Logic scheme of a Benes switch.

The Benes switch is composed by six elements: each of them has two inputs and two outputs and, depending on the voltage set, they have more power in one of the two output ports with respect to the other.
This elements can typically be built using Mach-Zehnder (MZ) interferometer or micro-ring resonator.
In this thesis the single element is a micro-ring resonator; more precisely two different types of rings have been studied: first e second order ring.

1.4 | Ring resonator

In this work the micro-ring resonator has been used as the atomic element in the Benes Switch.
The micro-ring has two optical input ports, two optical output ports and an electrical input port; the scheme is shown in figure 1.13.

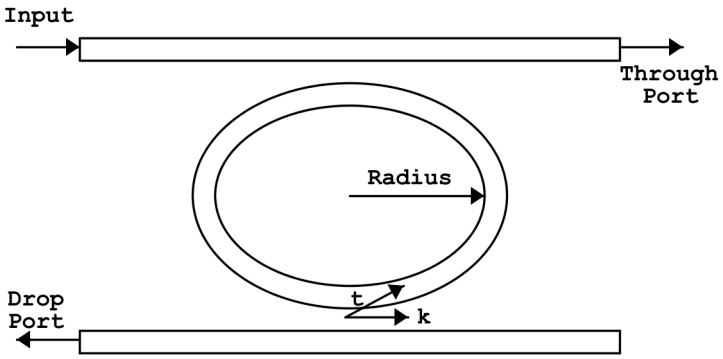

Figure 1.13: Scheme of a ring resonator.

t and k are the coupling coefficients and depend on the distance between the loop and the waveguide. In this thesis the ring is used to select in which of the two output ports most of the power at a certain frequency has to be directed. This is done applying a specific voltage in the electric port.

Analysis of RING FILTERS 2

A ring resonator, also known as micro-ring resonator, consists of a loop of optical waveguide with two directional couplers.
There are two main types of micro-ring: all-pass and add-drop. The difference is that the all-pass configuration has only one coupling waveguide, so only one input port and one output port; the add-drop configuration has two coupling waveguides, so it is a 2x2.

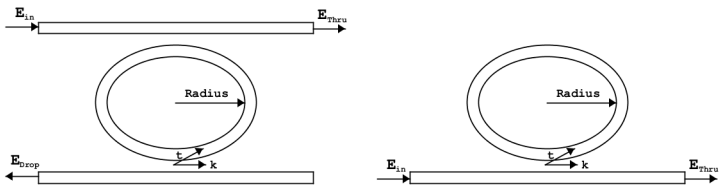

Figure 2.1: Left: Add-Drop configuration. Right: All-Pass configuration.

In this work the add-drop configuration has been used in order to have two input ports and two output ports.
The round-trip is given by:

$$L_{rt} = 2\pi r + 2L_c \tag{2.0.1}$$

where r is the radius of the internal loop and L_c is the coupler length that in this work is equal to zero.
The two signals from the two output ports are called Through and Drop as it is shown in figure 2.1 and they are given by [4]:

$$\frac{E_{thru}}{E_{in}} = \frac{-t_1 - t_2^* \sqrt{A} e^{i\phi_{rt}}}{1 - \sqrt{A} t_1^* t_2^* e^{i\phi_{rt}}} \tag{2.0.2}$$

$$\frac{E_{drop}}{E_{in}} = \frac{-k_1^* k_2 A^{\frac{1}{4}} e^{i\phi_{rt}}}{1 - \sqrt{A} t_1^* t_2^* e^{i\phi_{rt}}} \tag{2.0.3}$$

where ϕ_{rt} is the round trip optical phase and it is: $\phi_{rt} = \beta L_{rt}$; A is the power attenuation: $A = e^{\alpha L_{rt}}$; $t_{1,2}$ an $k_{1,2}$ are known as the point-coupling coefficients. For a symmetric design they are usually identical, i.e. $t_1 = t_2 = t$ and $k_1 = k_2 = k$.
The following relationship holds:

$$|k|^2 + |t|^2 = 1 \tag{2.0.4}$$

For an input signal with a narrower bandwidth,also a Micro-Ring resonator of the second order was designed. A second waveguide loop is added to the Ring described above and so the frequency response is multiplied by its self. In figure 2.2 the scheme of the Double Ring is displayed .

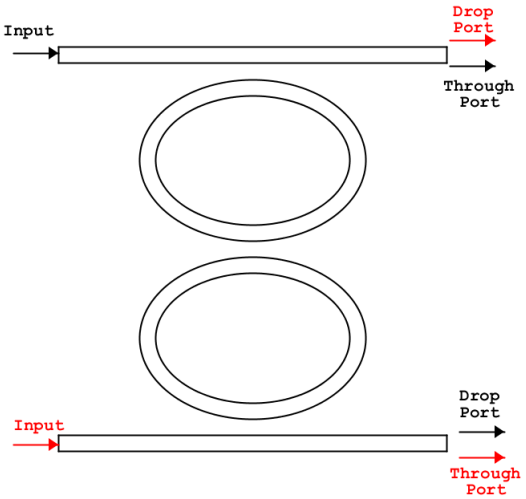

Figure 2.2: Scheme of the Double Ring.

Due to the second loop, unlike the first order ring, the two inputs are both on the left part and so connecting six rings for the Benes, the connections are like the ones in figure 1.12.
Adding a loop between the two waveguides allows to have a frequency response more symmetric in the two outputs; this means that in the Double Ring the drop port and the through port have the frequency response more similar each other but shifted by $FSR/2$. In this way the Drop port applies more attenuation in the wanted channels and consequently there is less attenuation in the through port.
The drawback of using this type of element is that being the duty cycle of the frequency response near to 50% the bandwidth is narrower. For this reason this device is a good option in the applications with an input signal with a narrower band.

2.1 | Physical Parameters

The parameters to be inserted in the model on the software OptSim have been calculated using the previous formulas.
To make the Benes work properly and to follow the channel grid shown in figure 1.8, the micro-ring must be resonant at one of the four central frequencies and it must have a FSR(Free Spectral Range) of 100 Ghz, that is the distance between two adjacent channels.
The parameters calculated are: the length of the ring L, the coupling coefficients k and t and the refractive index n_{eff}.
The length determines which will be the resonant frequency and the FSR. The coupling coefficients k and t determine the shape of the frequency response. Finally the refractive index n_{eff} can shift the spectrum, but it is given by the material used so it is a fixed parameter; in this case it is: $n_{eff} = 2.5$.

2.1.1 | Ring of the first order

Starting from the calculus of the length, to have resonance the following relationship must apply:

$$\frac{2\pi}{\lambda} n_{eff} L = 2\pi k \tag{2.1.1}$$

where k is an integer, given by

$$k = floor(\frac{2\pi}{\lambda} n_{eff} \frac{L_p}{2\pi}) = floor(\frac{n_{eff} L}{\lambda}) \tag{2.1.2}$$

In the previous formula λ is equal to c/f_1 and $n_{eff} = 2.5$. L can be calculated from the relation:

$$\frac{L n_{eff}}{\lambda_1 + \delta\lambda} = \frac{L n_{eff} + \lambda_1}{\lambda_1} L = \frac{\lambda_1^2}{\delta\lambda} \tag{2.1.3}$$

where for this work $\delta\lambda = c/(100\ GHz)$.
With the provisional value of L computed above, k can be calculated and finally the real value of the length is given by the formula 2.1.1, obtaining:

$$L_{final} = k \frac{\lambda_1}{n_{eff}} = 1.1979mm \tag{2.1.4}$$

with this value of L, the frequency response of the ring in the two ports with $t = k = 0.5$ is:

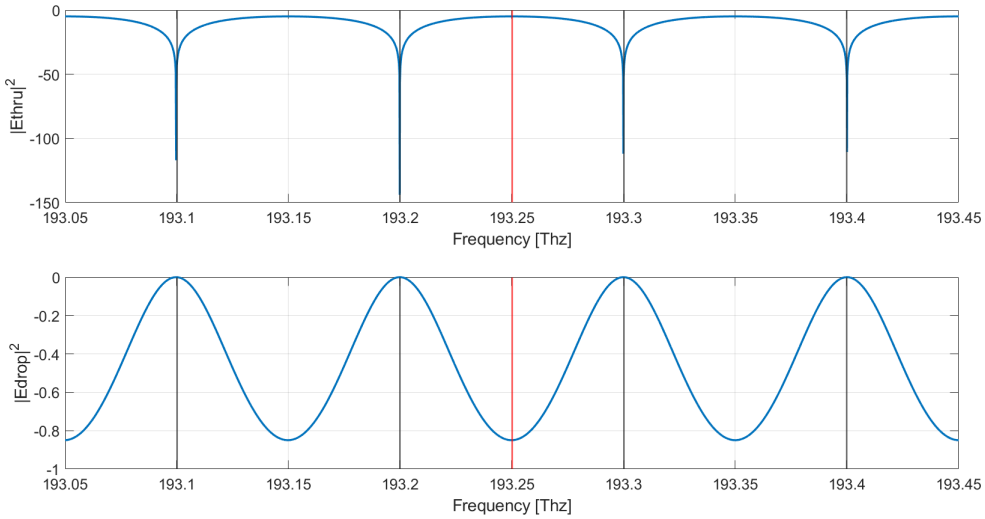

Figure 2.3: Frequency response of the ring normalized with the previously calculated parameters.

From the previous figure it is clear that in order to have better performance the bandwidth of the Drop port must be as large as possible. This is obtained changing the coupling coefficients t and k and setting them as: $t = 0.95$ and $k = 1 - t^2 = 0.0975$.

2.1.2 | Ring of the second order

Regarding the Double Ring, the length and the refractive index remain equal to the previous one. The main differences, concerning the design, are the coupling coefficients because in this case there are three couples of k and t instead of just two because there are three couplers: two that connect one loop with the external waveguides and one between the two loops. In figure 2.4 the three couples of coupling coefficients in the Double Ring scheme are shown.

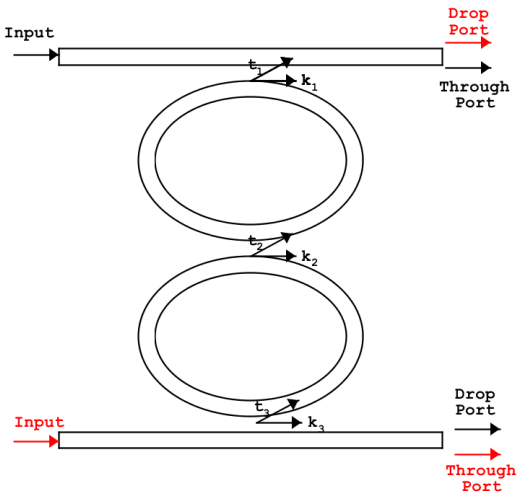

Figure 2.4: Coupling coefficients order in the Double Ring.

To maintain the symmetry, the first two couples t_1, k_1 and t_3, k_3 must be equal while the one in the middle, t_2, k_2, can be different from the others. The object is to have the two output spectra as similar as possible. After some simulations the results are:

- $t_1 = 0.95,\ k_1 = 0.0975$
- $t_2 = 0.75,\ k_2 = 0.4375$
- $t_3 = 0.95,\ k_3 = 0.0975$

2.2 | Voltage selection

From figure 2.3 it can be seen that just one of the two ports has the spectrum resonant at the working frequencies. The operation of the ring in this work is based on this principle.
Applying a potential difference on the electrical pin, the ring is heated and consequently the spectrum of both output ports is shifted. There is no difference if the voltage is negative or positive.
The ring can have two operating states that will be called Bar and Cross.

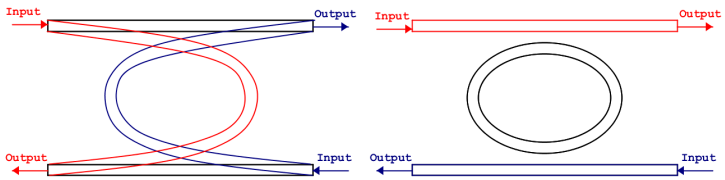

Figure 2.5: Left: Cross state. Right: Bar state.

In the Bar state there is no voltage, so the signal at one of the working frequencies in input is routed to the corresponding Drop port.
In the Cross state a specific voltage is applied to the heating port and so the spectrum is shifted; as a result the signal in input is routed to the corresponding Through port.
The higher the voltage, the more the spectrum is shifted so there is a specific value of voltage that moves the spectrum exactly of 50 Ghz. This value of voltage was found experimentally making different simulations for different values of voltage and for each of them calculating the minimum of one port and the maximum of the other.
The correct value is the one for which E_{drop} has the minimum at the working frequencies and E_{thru} has the maximum. The figure 2.6 shows the plot of the E_{drop} exported from OptSim, for different values of voltage.

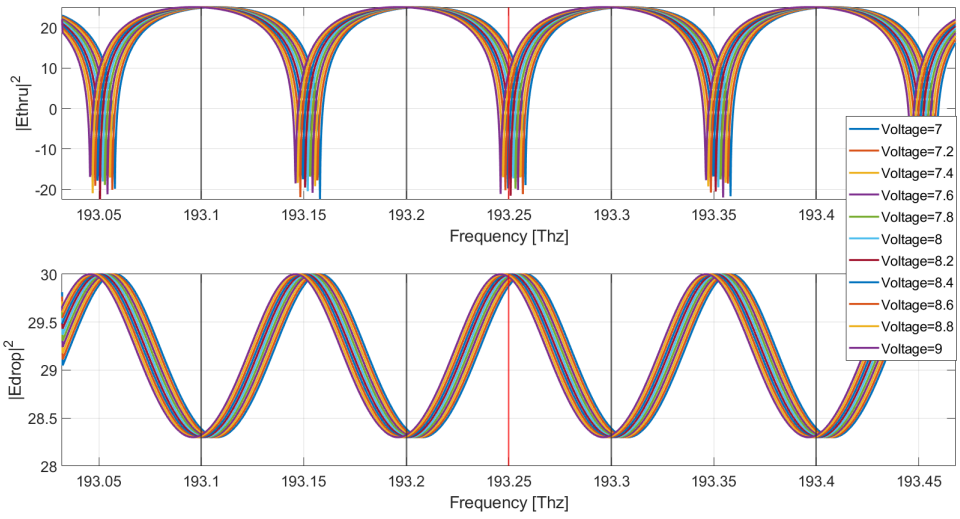

Figure 2.6: Frequency response of the ring changing the heating voltage from 7 V to 9 V.

From all simulated values, the voltage founded is equal to $V_h = 8.4$ V.

This result is also valid for the Ring of the second order because the frequency responses of the two loops are shifted with the electrical voltage a the same way of the previous one. The difference in this case is that there are two heating ports that to work properly must be excited with the same potential difference.

2.3 | Ring representation on OptSim

In order to simulate the behaviour of the ring, the software OptSim Circuit was used; OptSim Circuit enables the user to design photonic circuits using high-level symbols and to simulate them by taking into account bi-directional propagation of optical and electrical signals.
In this case a PDK was used inserting the previous calculated parameters:

- $L = 1.1979\ mm$
- $t = 0.95$
- $n_{eff} = 2.5$
- $V_h = 8.4\ V$

The block scheme of the ring used on the software is displayed in figure 2.7:

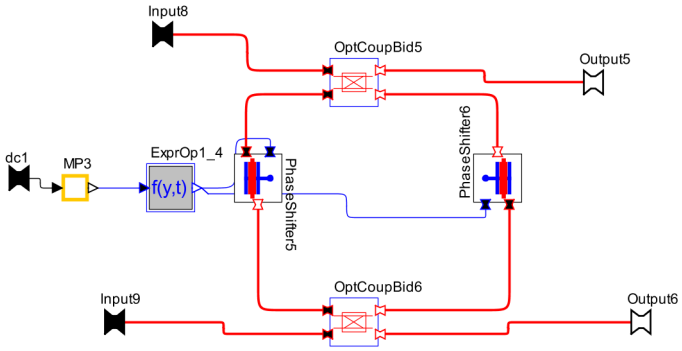

Figure 2.7: Block scheme of the ring simulated on the software OptSim.

In figure 2.7 can be seen the two couplers between the ports and the internal loop where the values of t and k are inserted .
The Phase Shifters in the loop take in input the heating voltage and shift the signal simulating the heating of the material.
Inserting four tags of the input and output ports, the software allows to incorporate all blocks shown in figure 2.7 and use it as single elements; an example can be seen in figure 2.8.

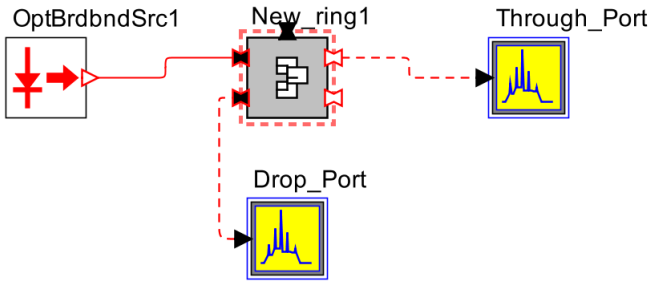

Figure 2.8: Block diagram used to simulate the single ring.

A PDK (Process Design Kit) is a library component that already has both circuit and layout representations. In some cases they are already in production in a factory so they are tested and certified.
In this thesis a custom PDK was used in order to adapt it to the needs of the work. Anyway, been a PDK, the ring used has already a mask for fabrication generated with the software OptoDesigner.

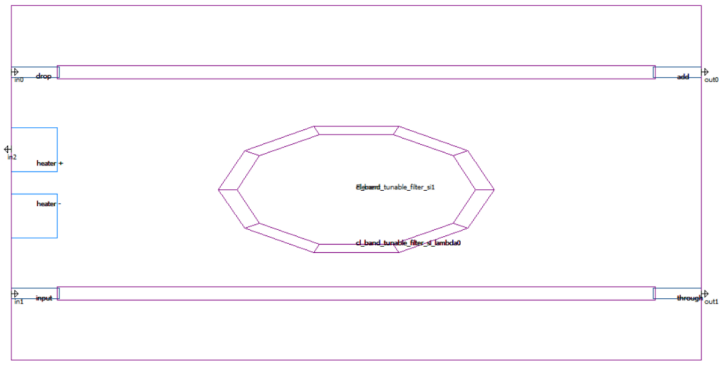

Figure 2.9: Mask for fabrication of micro-ring.

In figure 2.9 the mask for fabrication of the ring is shown where can be clearly seen the four optical ports and the input for the heating voltage.

Using the same blocks described above the Double Ring has been reported on the software OptSim.

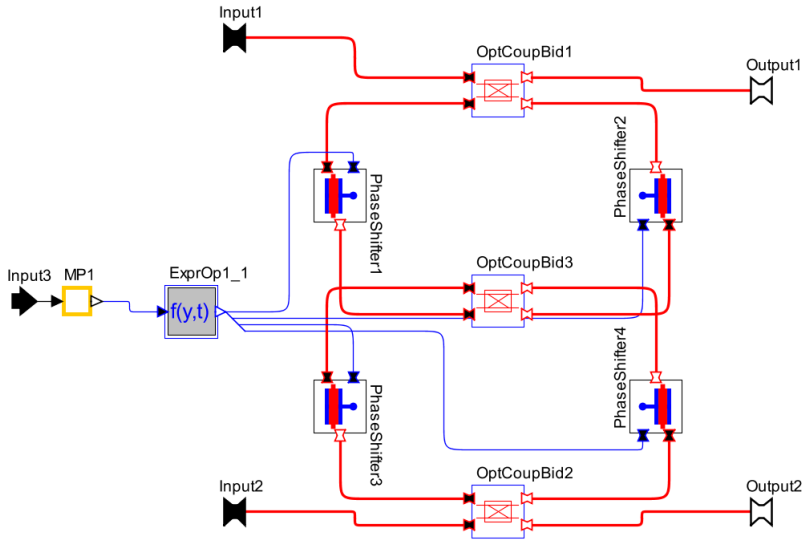

Figure 2.10: Bloch scheme of the second order Ring simulated on OptSim.

In this case there are three optical couplers, where the value of the coupling coefficients are inserted, and four phase shifters, in which the half of the loop length is inserted. All phase shifters are connected to the same heating port so during the simulation of the Benes they will be all subjected to the same voltage.
Another difference with respect to the first order Micro-Ring is that in this case the input ports are in the same side of the element; this is due to the paths that the input signals cross.

Analysis of a Benes Switch 3

3.1 | Examples of Benes Switch

There are many studies of this type of devices that differ in the number of elements, the application or the type of atomic element.

A first example is the Benes structure shown in in figure 3.1[1].

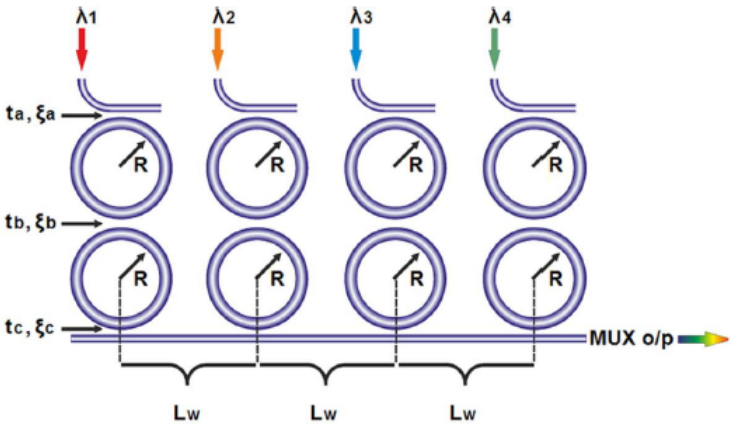

Figure 3.1: Example of Benes structure[1].

In this case there are 4 inputs, each one centered at a different frequency; the optical data is $40Gb/s$ NRZ. The channel spacing must be larger than 100GHz in order to enable high quality at the output.
This element is composed by four cascaded second order micro-ring resonators that allow to increase flexibility of the spectral filtering shape. All eight micro-rings have the same radius and are all connected to an electrical heating stage.
The first input signal at wavelength λ_1 is imported through the first second order Micro-Ring, then the signal is exported to its Drop port and arrives at MUX output after travelling through the Add ports of the subsequent three cascaded rings.
In a similar way, the second input signal at wavelength λ_2 emerges at the Drop port of the second Ring and reaches the MUX output after propa-

gating through the Add ports of the remaining two cascaded rings. The same procedure is repeated for wavelengths λ_3 and λ_4 entering the device through the subsequent second order MR modules, with the number of Add port transitions decreasing with increasing channel number.

Another example of structure of a Benes is shown in figure 3.2 [2].

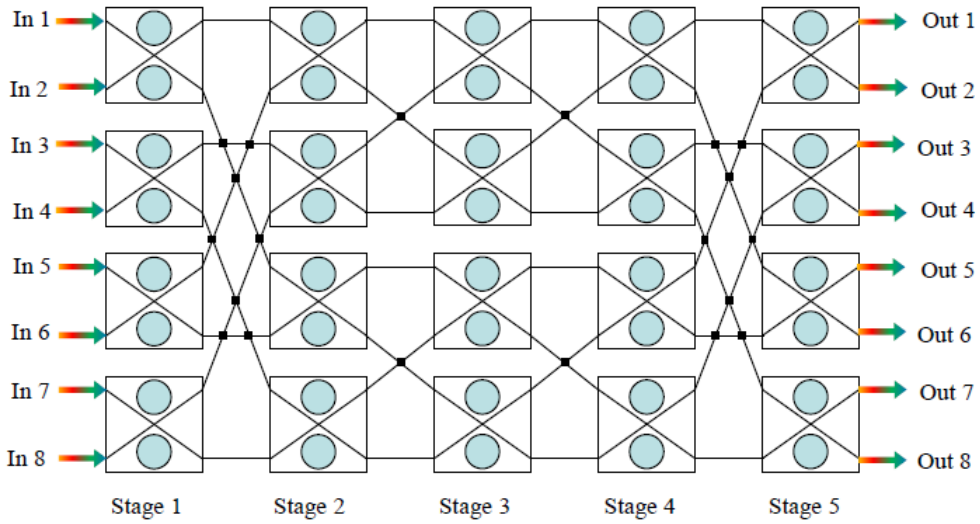

Figure 3.2: Example of Benes structure[2].

It is a 8x8 multistage switch with Benes topology.
In this example the single element is a second order micro-ring with a different layout with respect to the previous one. Here there are two waveguides crossing each other and two loops placed on two quarters. The layout is shown in figure 3.3

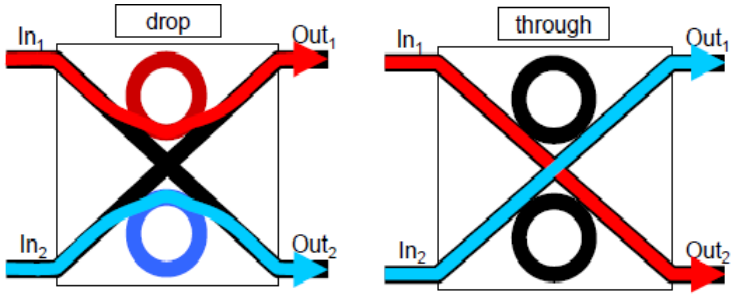

Figure 3.3: Second order micro-ring[].

As it shown in the figure above, there are two states of the ring and the passage from one to the other is decided by the electric voltage applied. The two loops must be controlled simultaneously, therefore being in "drop" state when both rings are in resonance and the state "through"

when both rings are off of the resonance.
This element is then inserted in the structure displayed in figure 3.2.

3.2 | Benes switch in this thesis

In this work a 4x4 Benes switch has been studied [3]. The main objective is, given in input four signals at different frequencies, direct each input to a specific output through the input electrical voltages.
The Benes is composed by six micro-ring described in the previous chapter; the structure is displayed in figure 1.12.
Exploiting the two states of each single ring (Bar and Cross) is possible to have a different combination of output changing the six voltages. There are two possible values of voltage (0V and 8.4V) and six electrical ports (one for each ring) so there are $2^6 = 64$ combinations. Obviously there are combinations of voltages with the same order of output but in this work will be analyzed all in order to see if there are better configurations.
To control the switch, it has been modeled with five matrices, one for each column of the rings and two that model the internal connections. In figure 3.4 is shown the scheme of the Benes with the corresponding matrices.

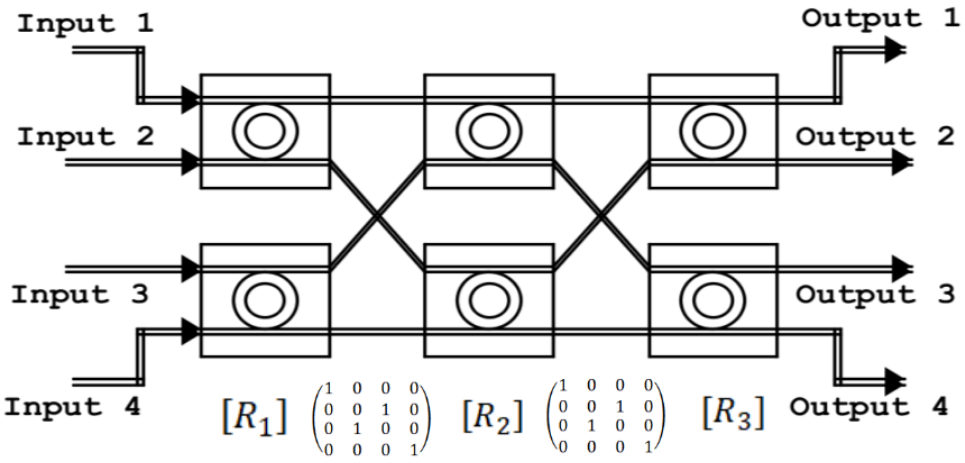

Figure 3.4: Benes switch with the corresponding matrices.

Each matrix has four rows and four columns; the rows represent the inputs while the columns represent the outputs.
The matrices that represents two vertical rings are:

- $[R_1]$: it represents the behaviour of the rings 1 and 4.
- $[R_2]$: it is for the rings 2 and 5.
- $[R_3]$: it describes the rings 3 and 6.

To better explain how these matrices are used, in figure 3.5 one column of the Benes composed by two rings is displayed .

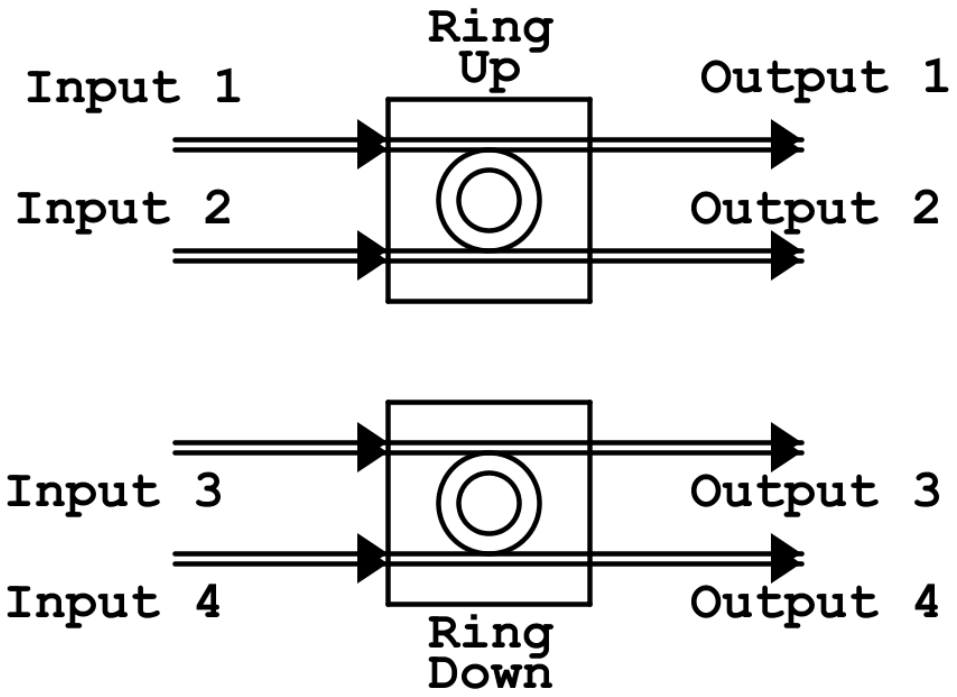

Figure 3.5: One column of the Benes composed by two micro-rings.

The ring in the top will be called Ring Up and the other will be called Ring Down; also the corresponding voltages will be called respectively V_{up} and V_{Down}.

Coming back to the matrices $[R_{1,2,3}]$, they can be assume four different configurations:

- $[R_{1,2,3}] = \begin{bmatrix} 1 & 0 & 0 & 0 \\ 0 & 1 & 0 & 0 \\ 0 & 0 & 1 & 0 \\ 0 & 0 & 0 & 1 \end{bmatrix}$: $V_{up}, V_{Down} = 0V$; both rings are in Cross state and the four inputs go through the corresponding Drop ports. From this matrix will be derived the next three cases. In figure 3.6 is shown the translation of the matrix in a graphically way.

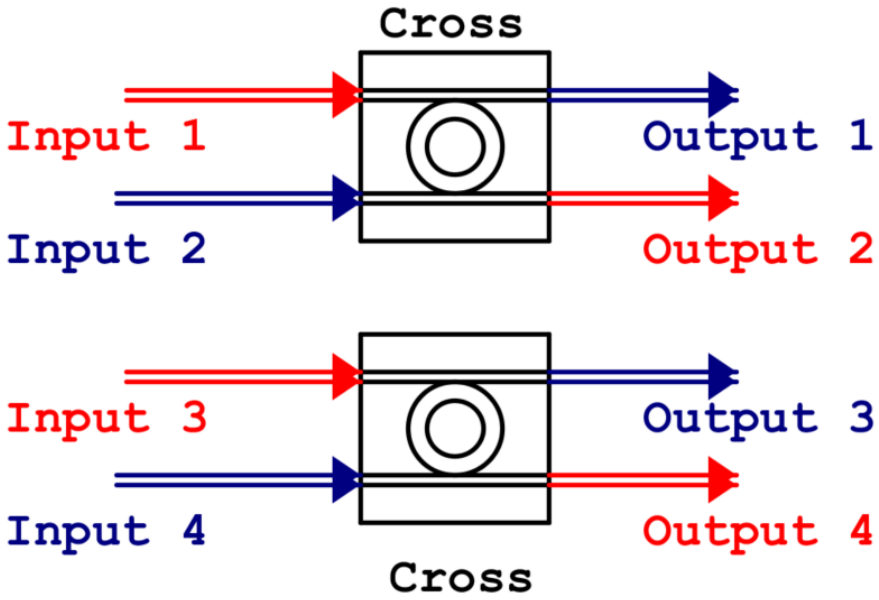

Figure 3.6: Cross-Cross configuration.

- $[R_{1,2,3}] = \begin{bmatrix} 1 & 0 & 0 & 0 \\ 0 & 1 & 0 & 0 \\ 0 & 0 & 0 & 1 \\ 0 & 0 & 1 & 0 \end{bmatrix}$: $V_{up} = 0V, V_{Down} = 8.4V$; in this case the Ring Up is in the same condition of the previous case so the two inputs are directed in the Drop ports; the Ring Down has the spectrum shifted due to the voltage equal to 8.4V so the two inputs are directed in the Through ports. Analytically, applying a voltage to the Ring Down means reversing the third row with the fourth row of the matrix of the previous case.

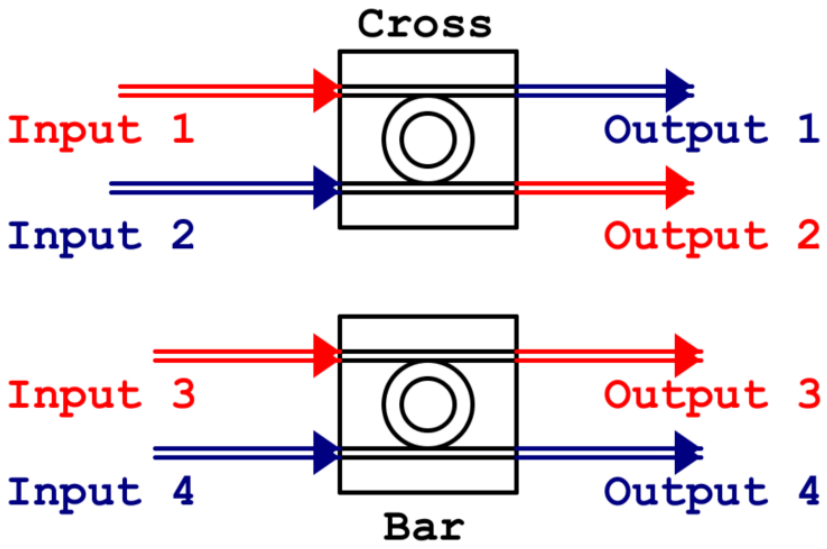

Figure 3.7: Cross-Bar configuration.

- $[R_{1,2,3}] = \begin{bmatrix} 0 & 1 & 0 & 0 \\ 1 & 0 & 0 & 0 \\ 0 & 0 & 0 & 1 \\ 0 & 0 & 1 & 0 \end{bmatrix}$: $V_{up} = 8.4V, V_{Down} = 0V$; this is the case opposite to the previous one so the Ring Up is in Bar state so in its electrical port there are 8.4V while the Ring Down is in Cross state. In this case the first row is reversed with the second one of the first matrix.

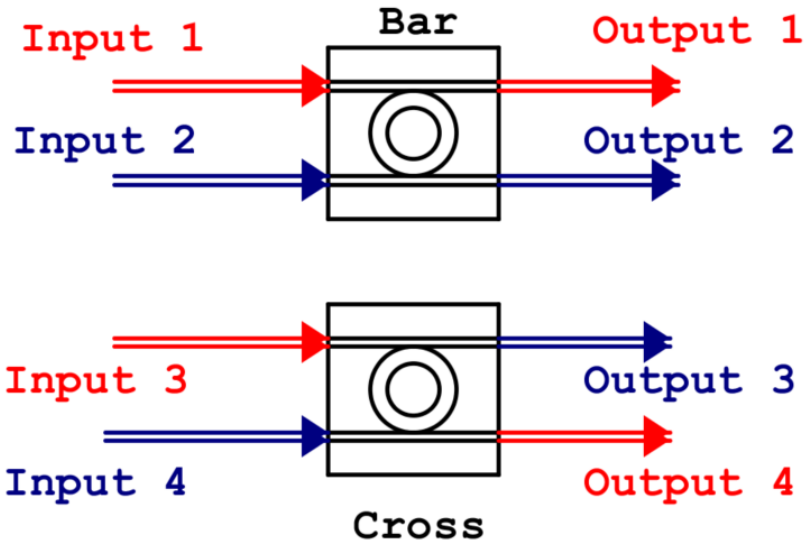

Figure 3.8: Bar-Cross configuration.

- $[R_{1,2,3}] = \begin{bmatrix} 0 & 1 & 0 & 0 \\ 1 & 0 & 0 & 0 \\ 0 & 0 & 0 & 1 \\ 0 & 0 & 1 & 0 \end{bmatrix}$: $V_{up} = 8.4V, V_{Down} = 8.4V$; in this last case both Rings are in Bar state so a voltage of $8.4V$ is applied to the electrical ports. This means that the four signals in input are directed to the corresponding through ports. This is the union of the two previous cases so the fourth row is reversed with the third and the first with the second.

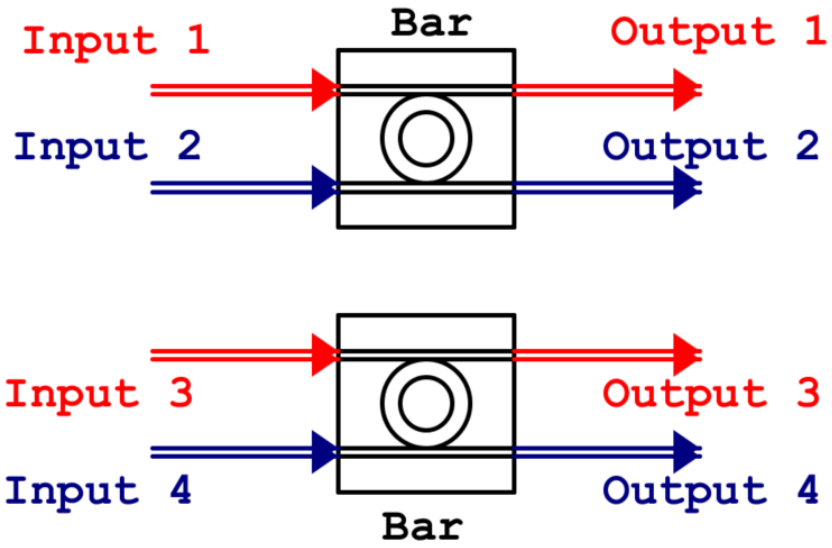

Figure 3.9: Bar-Bar configuration.

Between the three matrices described above there is also a 4x4 matrix: between $[R_1]$ and $[R_2]$ and between $[R_2]$ and $[R_3]$:

$$[M] = \begin{bmatrix} 1 & 0 & 0 & 0 \\ 0 & 0 & 1 & 0 \\ 0 & 1 & 0 & 0 \\ 0 & 0 & 0 & 1 \end{bmatrix} \tag{3.2.1}$$

It describes how the three columns of rings are connected each other. In the first row there is 1 in the first columns because the output 1 of a columns is the input 1 of the following column. In the second row there is 1 in the third column because the output 2 of a column of rings is the input 3 of the following one. The matrix $[M]$ takes into account the connections.

The use of this matrices to model the Benes allows to predict for each combination of voltages where the signals in input will be directed.
The equation used to analyze the behaviour of the Benes is:

$$[In_1 In_2 In_3 In_4] \cdot [R_1] \cdot [M] \cdot [R_2] \cdot [M] \cdot [R_3] = OutputSequence \tag{3.2.2}$$

Depending on the state in which $[R_1]$,$[R_2]$,$[R_3]$ are, the matrix product above will return a different combination of the inputs.

3.2.1 | Benes: Matlab

The matrix description of the Benes has been written on Matlab in order to automate the calculations and the iterations during the simulations. This description describes how the elements that composes the switch are connected each other.
The code used is the following

```
1
2  function [M_f]=Perm_func(RingsPerRow, RingsPerColumn
       )
3
4  Input=1:RingsPerColumn*2;
5  NumRings=RingsPerColumn*RingsPerRow;
6  Permute=@(A,r)A([1:r-1,r+1,r,r+2:end],:);
7  Y=eye(length(Input));
8  MSwitch=Permute(Y,2);
9  Res=zeros(2^NumRings,NumRings+RingsPerColumn*2);
10 for k=0:2^NumRings-1
11     for kr=1:RingsPerRow
12         M(:,:,kr)=Y;
13     end
14     States=dec2bin(k,NumRings)-'0';
15     for kr=1:NumRings
16         c=rem(kr-1, RingsPerRow)+1;
17         r=fix((kr-1)/ RingsPerRow)*2+1;
18         if States(kr)==0
19             M(:,:,c)=Permute(M(:,:,c),r);
20         end
21     end
22     Output=Input*M(:,:,1);
23     for kr=2:RingsPerRow
24         Output=Output*MSwitch*M(:,:,kr);
25     end
26     Res(k+1,:)=[States, Output];
27     M_f(k+1,:)=[k, States, Output];
28 end
```

This is a general code to create the scheme described above but it can be used also for a different number of elements. It is a function that takes in input the number of rows and columns. The function calculates the matrix product and it return a table. A small extract of the result is reported in figure 3.10

NUMBER	Vh1	Vh2	Vh3	Vh4	Vh5	Vh6	InPort1	InPort2	InPort3	InPort4
0	0	0	0	0	0	0	3	4	1	2
1	0	0	0	0	0	1	3	4	2	1
2	0	0	0	0	1	0	1	4	3	2
3	0	0	0	0	1	1	1	4	2	3
4	0	0	0	1	0	0	4	3	1	2
5	0	0	0	1	0	1	4	3	2	1
6	0	0	0	1	1	0	1	3	4	2
7	0	0	0	1	1	1	1	3	2	4
8	0	0	1	0	0	0	4	3	1	2
9	0	0	1	0	0	1	4	3	2	1
10	0	0	1	0	1	0	4	1	3	2
11	0	0	1	0	1	1	4	1	2	3
12	0	0	1	1	0	0	3	4	1	2
13	0	0	1	1	0	1	3	4	2	1
14	0	0	1	1	1	0	3	1	4	2
15	0	0	1	1	1	1	3	1	2	4
16	0	1	0	0	0	0	3	2	1	4

Figure 3.10: Part of the table obtained from the function "Perm func".

The table is composed by 64 rows (2^6 = all possible combination of the six voltages) and 13 columns. From the second to the seventh column are respectively the voltage in the first ring up to the voltage to the sixth ring. In the first column there are the equivalent numbers in decimal of the binary number formed by the 6 voltages columns.
The columns $InPort_{1,2,3,4}$ are dedicated each one to an input port; for example the number 3 in the column $InPort_1$ means that the input in the port 1 will be directed in the $OutPort_3$.
Modelling the Benes in matrix form allows to simplify the simulation process; there is no need to change the six voltages to change the configuration but can be simply selected one row of the previous table. For each configuration its not enough to change the voltages because also the resonant frequency of the four receivers must be changed in order to calculate correctly the BER (Bit Error Rate).

3.2.2 | Benes: OptSim

As for the ring, the Benes switch has been reported in the software OptSim connecting six of the ring described in the Chapter 2. In figure 3.11 the scheme of the ring in the software is shown.

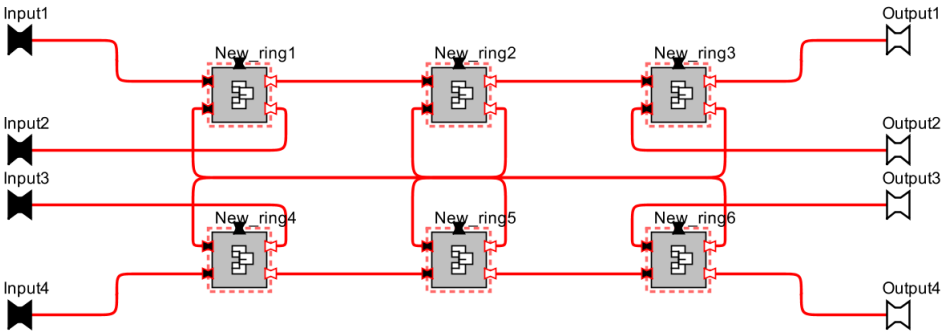

Figure 3.11: Block scheme of the Benes switch used for the simulations.

The scheme is slightly different from the one displayed in figure 1.12 because to clarify the two inputs were set both on the left but in reality two inputs in the micro-ring are in opposite positions; anyway the connections are the same described above.
Being used a series of PDKs, also in this case a fabrication mask has been generated and it is shown in figure 3.12

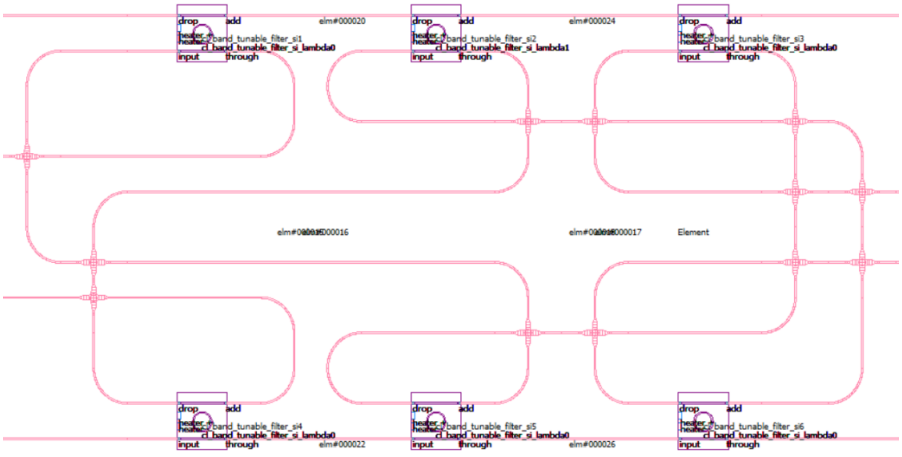

Figure 3.12: Mask fabrication of the Benes switch used.

Another device simulated is the Benes built with the second order Micro-Ring. It is based on the same principle of the previous one and the main difference is that in this case each element have the output ports in the same part instead of being in opposite positions. In figure 3.13 the OptSim scheme of the Benes Switch is shown .

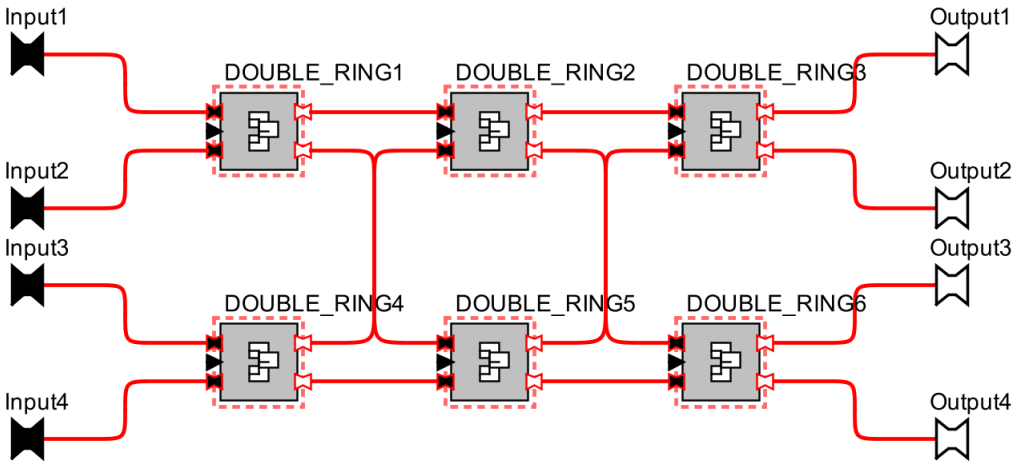

Figure 3.13: OptSim scheme of the Benes using the Second order Micro-Ring.

As for the Transmitter and the Receiver, the scheme of the Benes Switch has been saved in a different file from that one used to make simulations in order to have just one block that takes in input the parameters. In figure 3.14 the block scheme used to study the behaviour of the device is displayed.

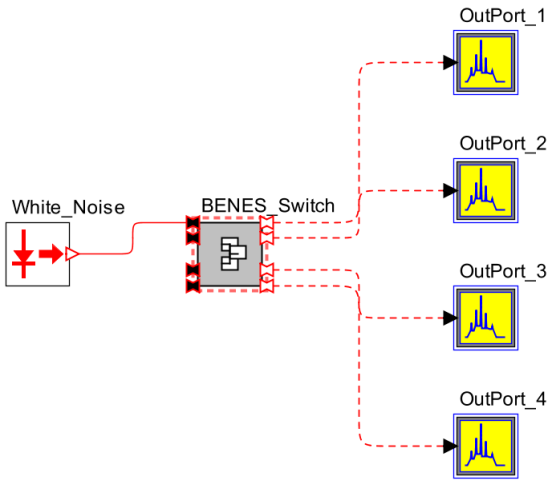

Figure 3.14: Blocks used to study the Benes.

The input block is a noise generator that has a flat frequency shape at 30dB in all simulation band; in this way the outputs of the Benes represents the frequency response.
Obviously there is a different frequency response for each combination of

voltages but for example the situation with all voltages equal to 0V has been analyzed and reported here.
To find out where each input will be directed is enough to make the matrix product described above; given an input sequence the output sequence is:

$$\begin{bmatrix}1 & 2 & 3 & 4\end{bmatrix} \cdot [R_1] \cdot [M] \cdot [R_2] \cdot [M] \cdot [R_3] = \begin{bmatrix}3 & 4 & 1 & 2\end{bmatrix} \tag{3.2.3}$$

This means that when all voltages are 0V, the signal in the input port 1 will be founded in the output port 3; the signal in input 2 will go in output 4 and the same for the other two signals.
To demonstrate this, in figure 3.15 a 4x4 graph is shown, where are displayed different frequency responses of the Benes when all voltage are equal to 0V.

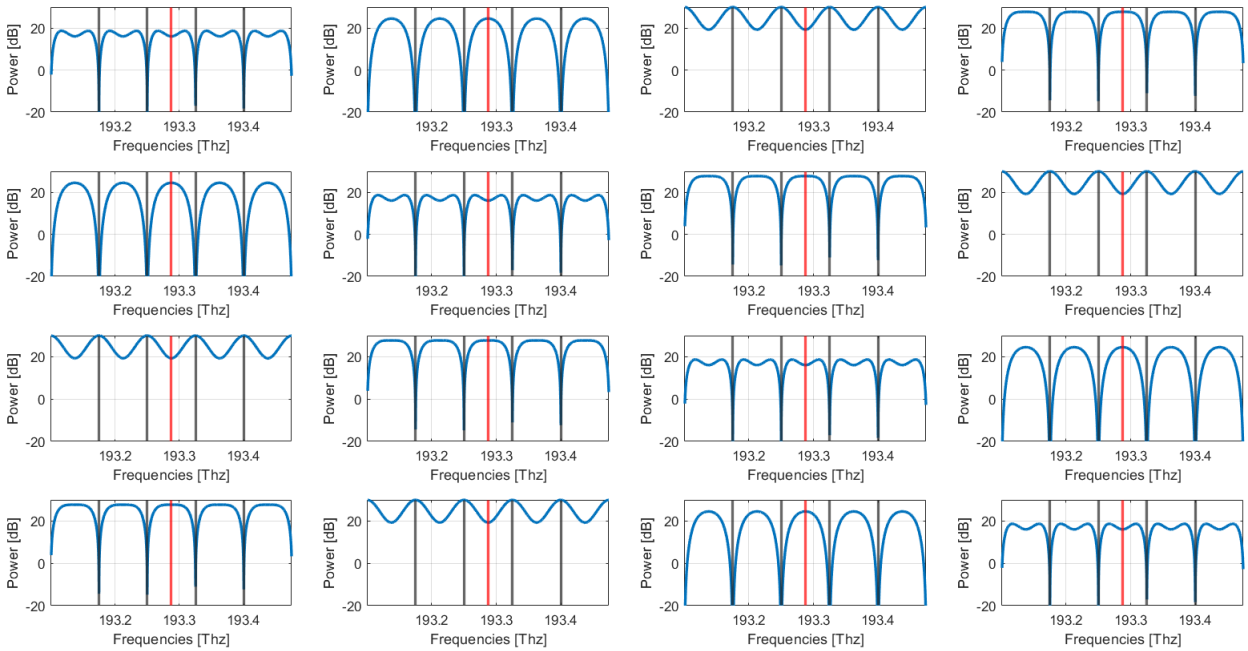

Figure 3.15: Frequency response of the Benes with all voltage equal to 0V.

The columns represent the inputs and the rows represents the outputs so, for example, the graph in position (1,1) represents the frequency response in the output port 1 when the white noise is in the input port 1. In this condition is clear that the only four graphs with a curve resonant at the working frequencies are (1,3), (2,4), (3,1) and (4,2); this is perfectly consistent with the result obtained in the matrix product 3.2.3. Moreover this sequence is the same shown in figure 3.10 where the first row represents exactly this case.

Once analyzed the frequency response, four TXs have been added in input and four RXs have been set in output. The important thing is that the transmitter must resonate at four different frequencies in order to not have interference inside the Benes.
Also in the receiver must be set a resonant frequency of the internal laser in order to demodulate correctly the signals but for each combination of the voltages the output order of the signals is different. To know where a specific signal will go, the table generated from the function "Perm_Func" is used looking at the last four columns of the generated table.
The figure 3.16 shows the OptSim window with the Benes, four Transmitters, four Receivers and eight spectrum plot in output of the Transmitters and the Benes.

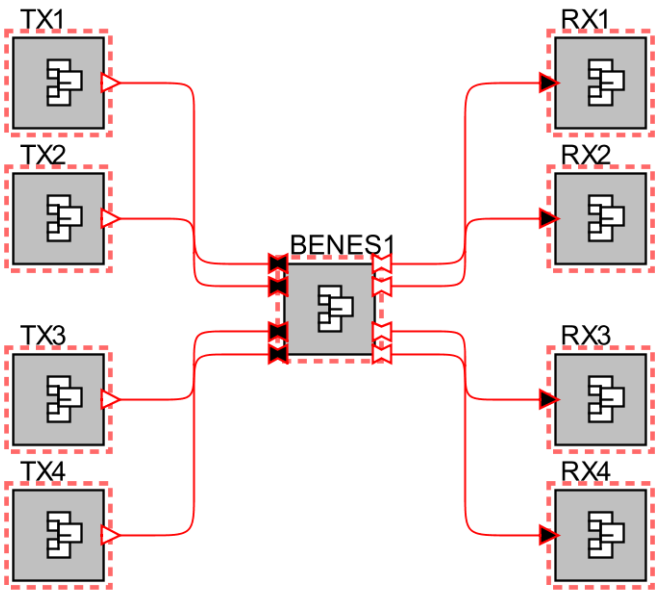

Figure 3.16: Blocks used to simulated the entire system.

Each TX block calls a MatLab function to generate the input bit sequence; in the RX block the signals, after passing through all the blocks of figure 1.11, are saved in a MatLab Workspace. To obtain the final result in terms of BER, the saved Workspace must be elaborated from another Matlab function that calculates the Bit Error Rate of each Receiver and the corresponding constellation of x-polarization and y polarization.

4 Analysis of the impact of Benes Switch on a system performance

In this chapter, the different simulations made on the system are described.
The first element to be analyzed is the micro- ring; once all parameters were calculated as described in Chapter 2, it was inserted in OptSim and characterized by means of the $H(f)$ with a white noise generator in input.
Then the micro-ring was used to construct the Benes structure connecting six of them together. Considering the white noise source, the transfer function of the Switch was studied verifying that the behaviour was the same described in matrix form.
Finally the Transmitters and Receivers were added to the system in order to verify if the Benes worked properly in terms of BER and not only in terms of the frequency response.

4.1 | Characterization of Micro-Rings filters

The most important features that the Micro-Ring must have are:

- Resonance at all the working frequencies.
- Free Spectral Range (FSR) equal to the distance between two working frequencies.
- Bandwidth as large as possible.
- With a pre-defined voltage of 8.4 V it should its state from Cross to Bar and so shift the spectrum of half of the FSR.

Regarding the first three conditions, they can be verified through the graph in figure 4.1

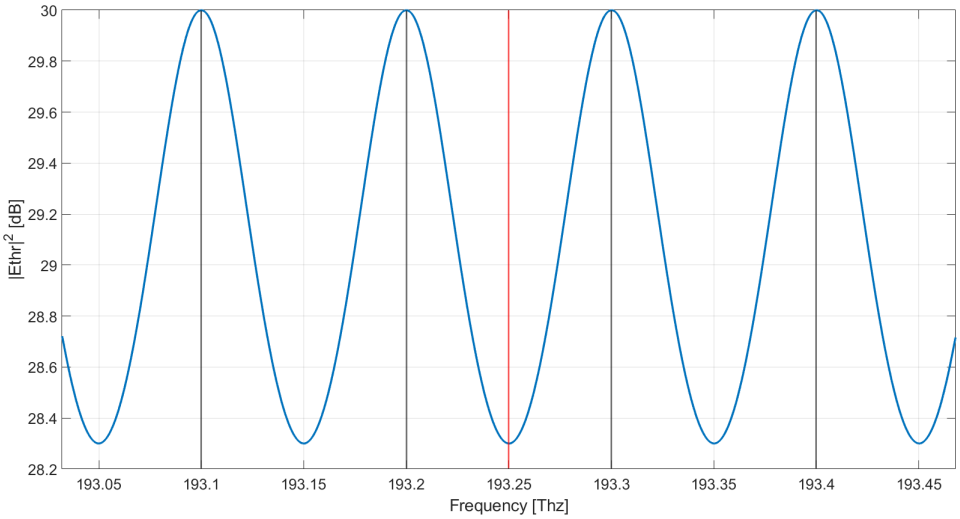

Figure 4.1: Frequency response of the ring of the Drop Port.

The curve have its maximums at the four working frequencies (black vertical lines), therefore both the first and the second conditions are verified. Regarding the Bandwidth, the coupling coefficients are as large as possible so it cannot be larger than this.
Figure 4.2 shows two curves: one is the output of the Drop port when the ring is in Cross state, while the other is the output when the ring is in Bar State.

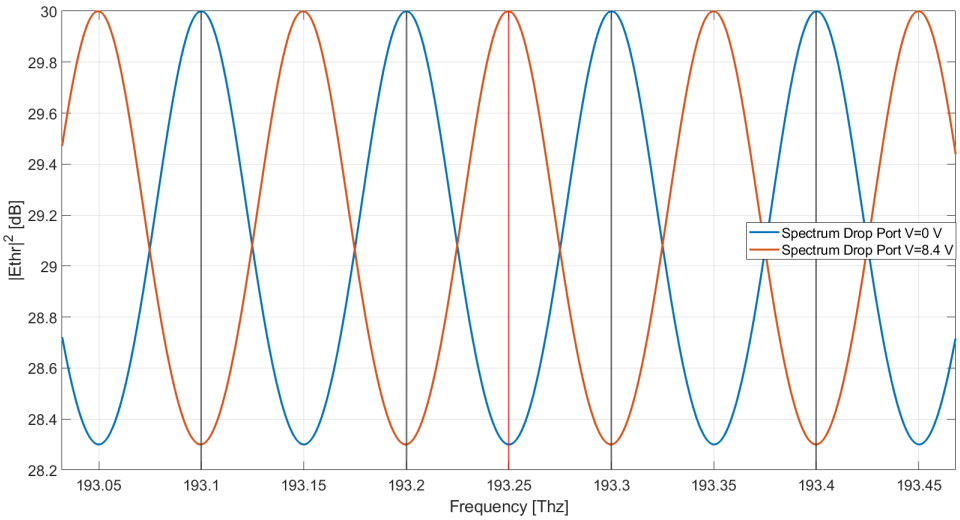

Figure 4.2: Comparison between Cross state and Bar state in the Drop Port.

When the Ring is in Cross state the Drop Port has its maximums at the

working frequencies, while when it is in Bar state its minimums are at the working frequencies.
To confirm this observation and to be more clear, in figure 4.3 the plot of the Through Port is shown in the same condition of figure 4.2.

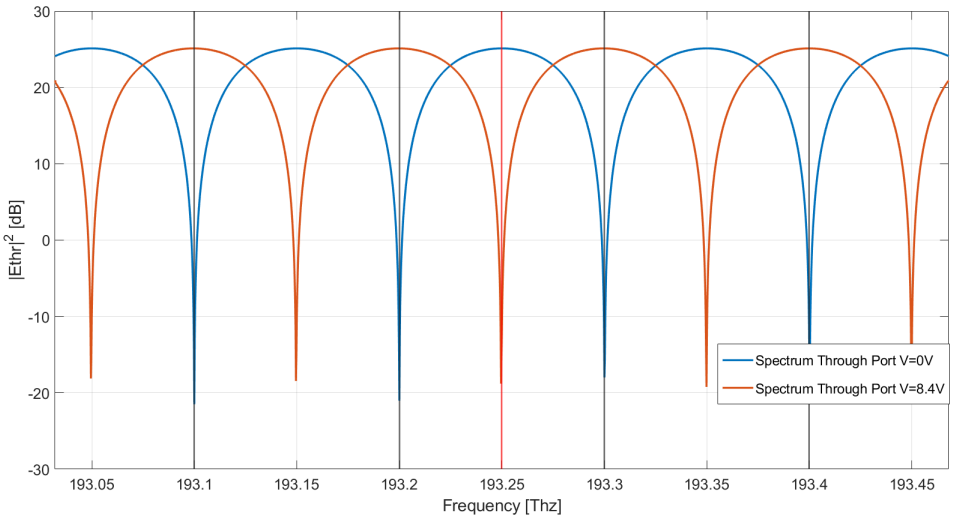

Figure 4.3: Comparison between Cross state and Bar state in the Through Port.

In this case the maximums are at the working frequencies in the Bar state instead of the Cross state. This is the expected result because in this way the power is routed to a different port depending on the voltage in the heating port.
The Drop port has a small variation between the maximum and the minimum; it allows the signal to pass through this port even if the band is not large as the bandwidth of the signal.
The through port instead has a large variation between maximum and minimum and it has a large bandwidth. The negative side of the transfer function of this port is that there is an insertion loss effect.

4.2 | Characterization of the Double Micro-Ring

The Ring of the second order must have the same features of the previous one so:

- Resonance at all working frequencies.
- Free Spectral Range (FSR) equal to the distance between two working frequencies.
- Bandwidth as large as possible.

- With a voltage of 8.4V it must change its state from Cross to Bar and so shift the spectrum of half of the FSR.

An additional requirement for this type of ring is that the Drop Port must have higher attenuation between two working frequencies in order to have more power in the other port. This allows to reduce the attenuation in the Through Port and so to have a better performance in the Receiver when the signal is demodulated.
As for the previous Ring, the first three conditions can be verified in the frequency response of the Drop port, displayed in figure 4.4.

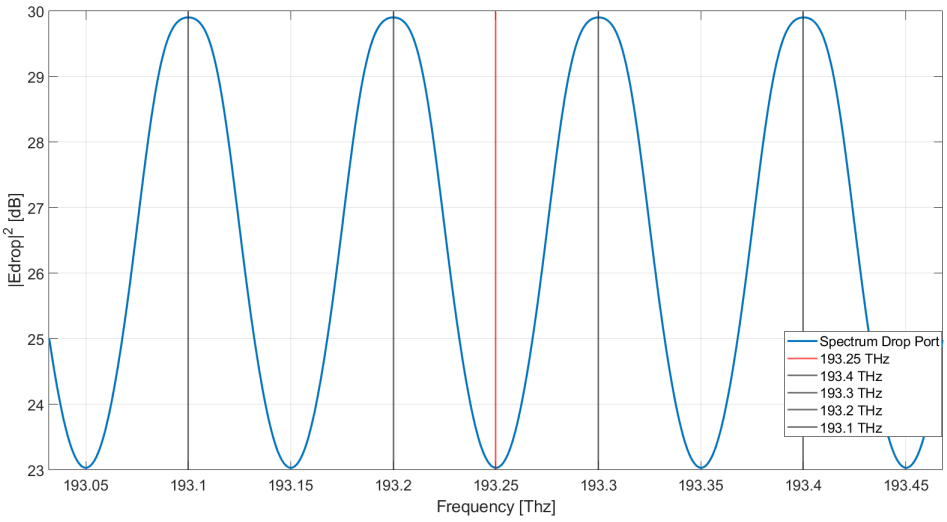

Figure 4.4: Frequency response of the Drop Port of the Double Ring.

It is clear that also in this case the conditions are respected because the frequency has its maximums in the four working frequencies and so it has a FRS equal to 100 GHz.
In order to verify the last condition, the Drop and the Through Port spectra are shown in the following figure.

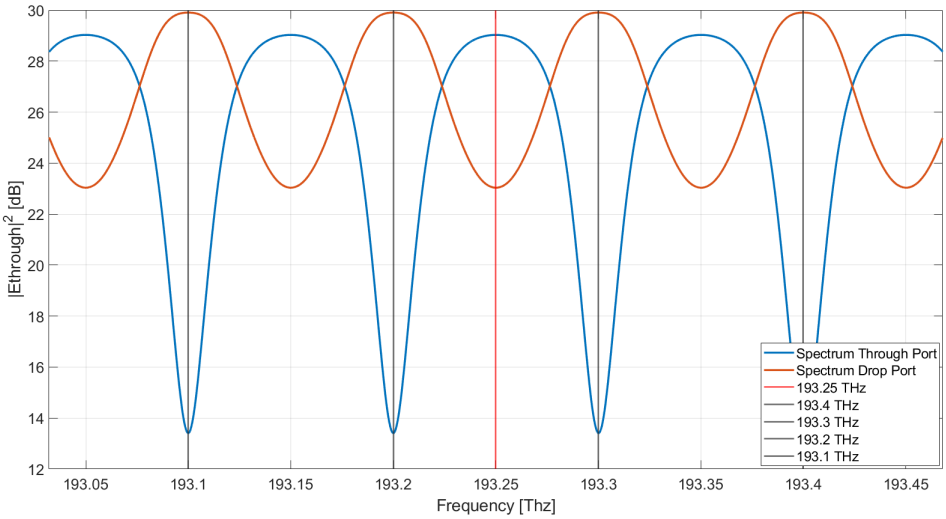

Figure 4.5: Frequency response of both ports of the Double Ring.

Even if the two frequency responses are not identical, there is anyway more symmetry with respect to the case with just one Ring. This allows the Benes Switch to work better, attenuating in the correct channels and not wasting too much power in the channels that need it instead.
The negative aspect is that now, being the two frequency responses more similar, there is less band available to transmit the signal.
For this reason, this type of device is optimum in the applications where the input signal has a band narrower than 32 GHz.

4.3 | Characterization of the Benes Switch

The main condition that the Switch must respect is that, given four input signals, resonant at four different channels, it should be able to send each input in any of the output port. In order to know which will be the Out-port, given a specific input, it is sufficient to use the IN-OUT table conversion described above.
In figure 4.6 a matrix of transfer functions of $H(f)$ is shown. The 16 graphs were obtained with all voltages are equal to zero; these spectra correspond to the first case of the table generated by the MatLab function described above.

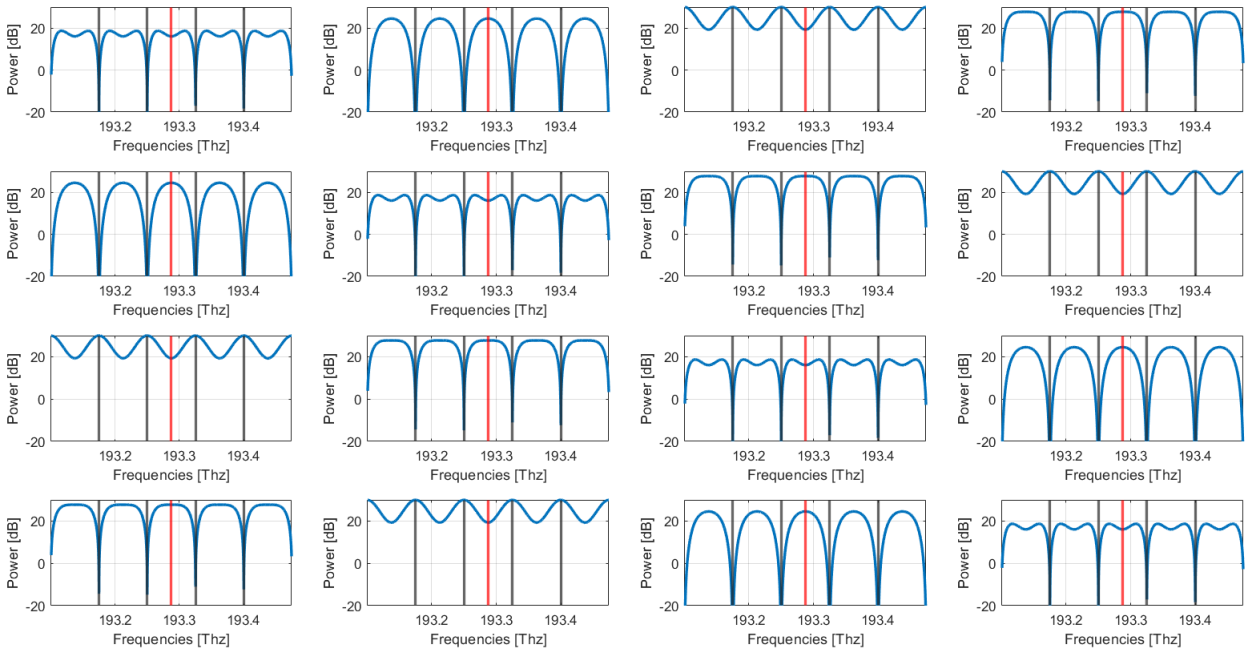

Figure 4.6: Matrix of frequency responses of the Benes Switch with all voltage equal to 0 V.

In this figure a symmetry between the four ports can be noticed in the graphs; for each graph in a row, it is possible to find another identical one in another row.
Furthermore, the graphs along the two diagonals are the same.This is due to the fact that all rings are in Cross state and it is not present in the others cases except for the last one.
The case number 64, when all driving voltages are in 'High' stats, is the opposite of this one so all rings are in Bar state and the equivalent subplot is shown in figure 4.7.

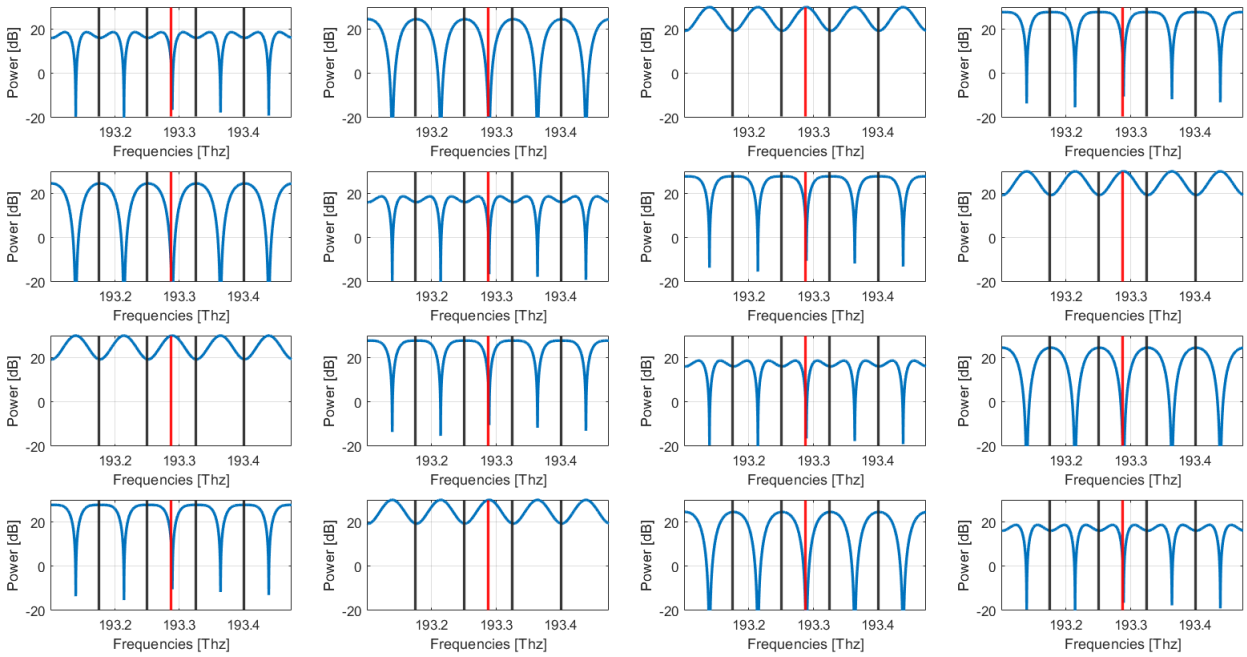

Figure 4.7: Frequency response of the Benes with all voltage equal to 0V.

Also in this case there is a symmetry along the two diagonals. More precisely in figure 4.7 the graphs are the same as in figure 4.6, but all shifted of $FSR/2$. In this case it is more clear how the customization of the Micro-Ring has direct effects on the response in the Switch at higher level.
Figure 4.8 shows the direct comparison of the base graphs, repeated in each row, of figure 4.6 and 4.7.

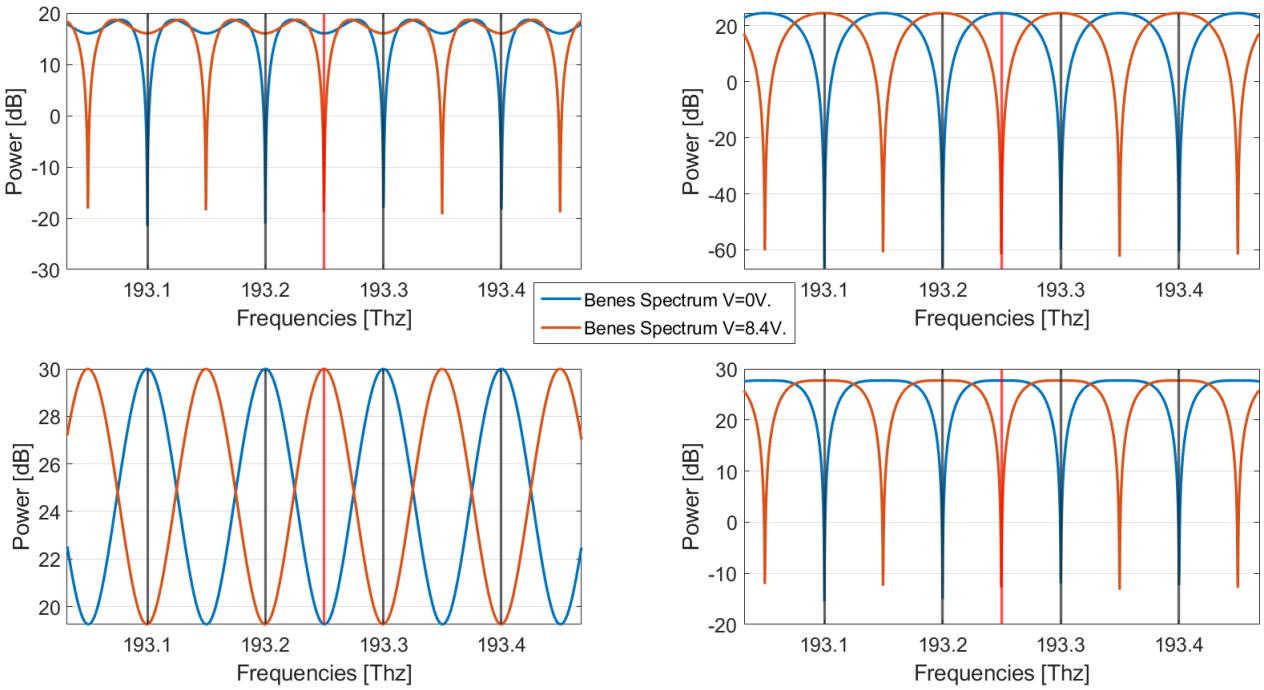

Figure 4.8: Comparison of $H(F)$ of the Output ports of Benes Switch with V=0 V and V=8.4 V.

As for Ring Filters, also in this case, looking at the graph in position (2,1), the curves for 0V (blue) and 8.4V (red) have respectively the maximum and the minimum at the four working frequencies.

The Benes Switch has been simulated also using the Double Ring. In this case the requirements are the same of the previous case so the bandwidth should be large enough to allow the input signal to pass. Regarding the maximums in the four channels, they are guaranteed by the design and the verification of the ring that composes the structure. In figure 4.9 the subplot of the four output ports is displayed when there is a flat white noise in input in the port 1.

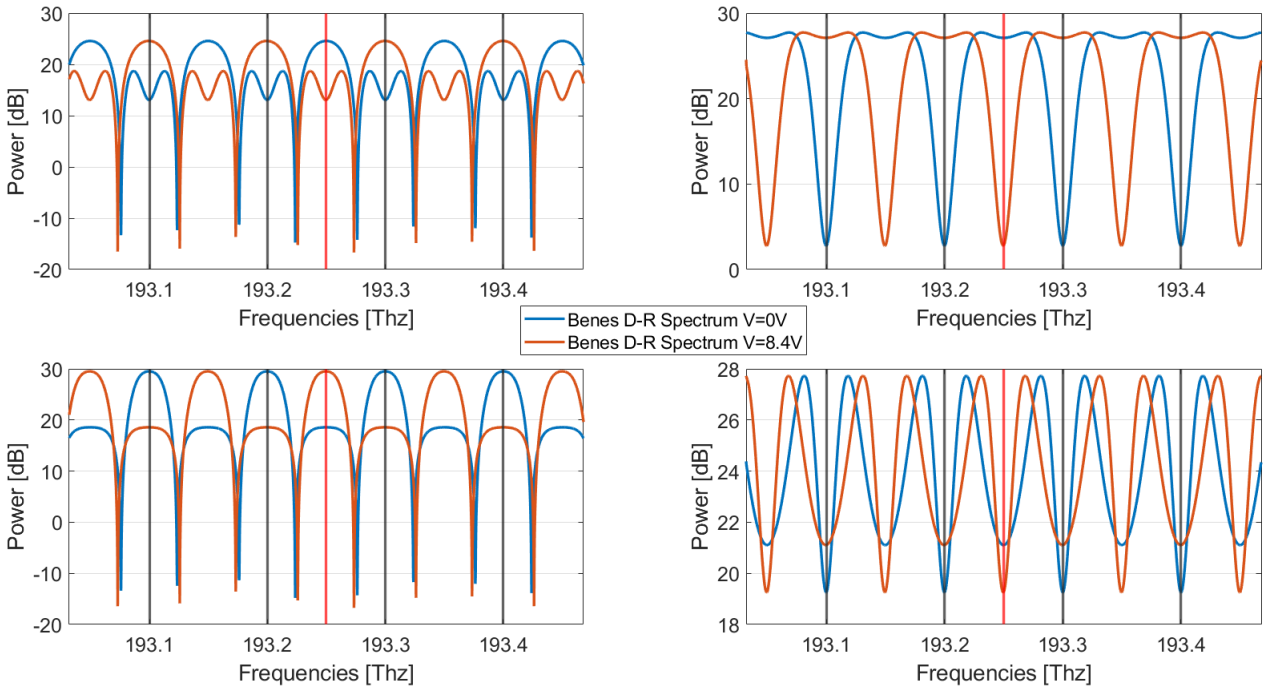

Figure 4.9: Comparison of Benes Switch output between V=0V and V=8.4V.

In the figure above an white noise source is connected to the port 1 of the Benes Switch. The same results shown in the previous figure can be obtained if the white noise is sent to any of the other three ports.
From the figure above it is clear that the Double Ring has the expected effect because in this case the available band is narrower so the input spectrum must occupy a narrower band. The positive aspect is that there is less attenuation in the other port and it will be translated in an higher BER (Bit Error Rate).

4.4 | Evaluation of the impact on system performance.

Once the behaviour of the Benes Switch was verified, the work has risen to a higher level inserting a Transmitter in the inputs and a Receiver in the outputs .
The objective is to calculate which is the penalty in terms of OSNR (Optical Signal to Noise Ratio) given a BER target.

4.4.1 | Frequency Shift

In this thesis, a WDW signal is used as input of the device with 4 different lambda centered in four different channels. The four components are then divided in order to send to each port of the Benes Switch one lambda. In figure 4.10 is shown the spectrum of the signal in input of one port at 32 GBaud.

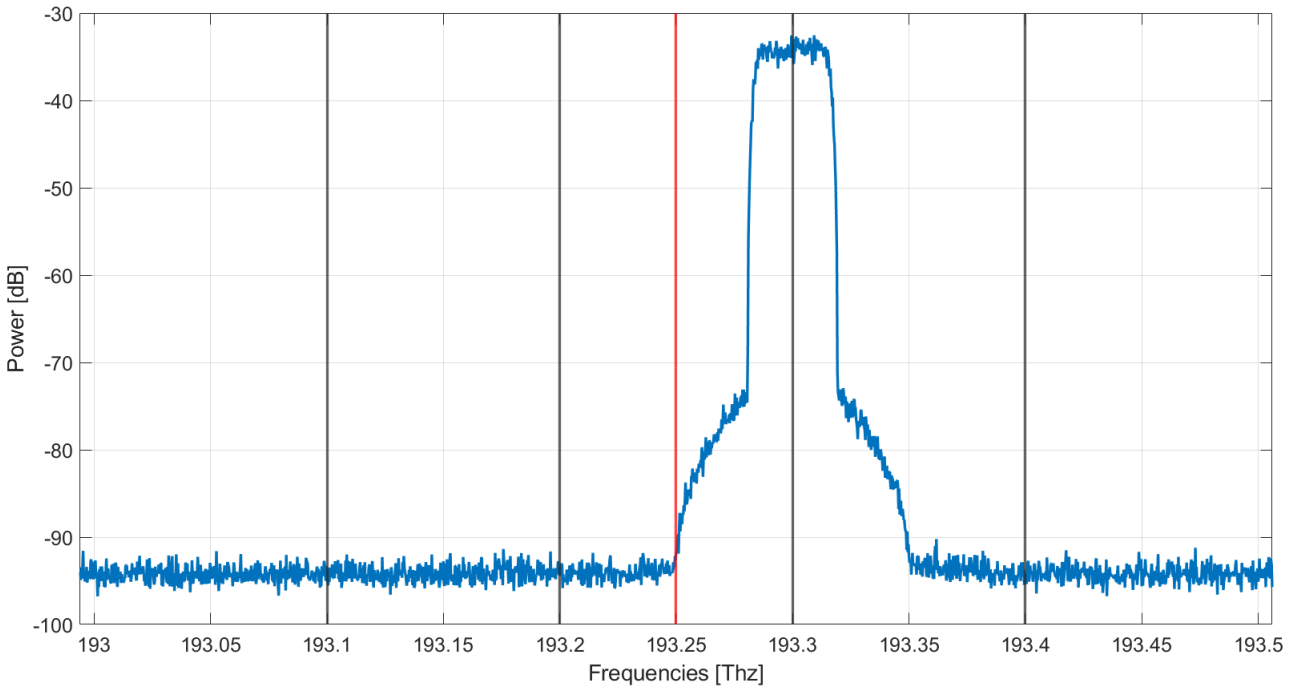

Figure 4.10: Raised Cosine transmitted at 32 GBaud at one of the working channel .

The figure 4.11 shows the signal in input of the Benes Switch composed by the Rings of the first order.

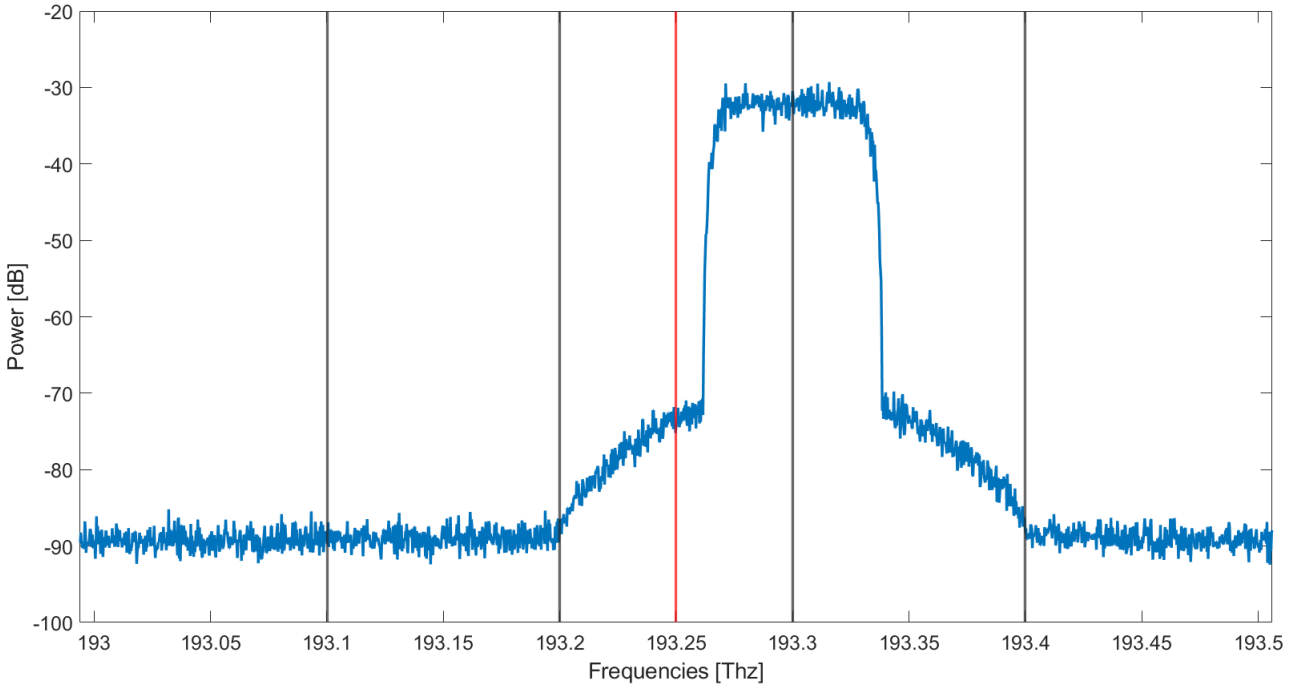

Figure 4.11: Raised Cosine transmitted at 64 GBaud at one of the working channel.

4.4.2 | Filter/Power Normalization

Over the Benes, the four TX blocks and four RX blocks, four equal additionals blocks have been added; each of them are composed by a filter and a power normalizer. This is needed because in addition to the filtering effects, the Benes composed by the first order rings introduces in the signals also an attenuation effect. In order to take into account only the filtering effect, the channel under test is isolated with the filter in order to remove the unwanted components; before entering the Receiver, the power of the filtered signal in normalized to 0 dBm eliminating so the power reduction.

4.4.3 | Simulation Framework

In this work many simulations were made in order to characterize the Benes Switch and to study which is the penalty in terms of bit counting due to the switch. To make this characterization, the six voltages of the Rings, the frequencies of the receivers and the OSNR needs to be changed in an easy way. The scan of a variable on the software OptSim was used initially to make the simulations with a variable OSNR, with a single configuration of the six voltages; this allowed to measure the

OSNR penalty. A more controllable tool was needed to run all simulations.
The OptSim file are written with the .moml extension; it is a Modeling Markup Language Document. MoML is an XML modeling markup language. It is intended for specifying interconnections of parameterized, hierarchical components.
The changing of the variables was done changing the OptSim (.moml) source file of the simulation ad inserting the wanted values in the variables.
The steps to follow are:

1. Each variable that has to be changed must be defined in the symbols section of OptSim.

Parameter	Value
Vh1	Volt1_R
Vh2	Volt2_R
Vh3	Volt3_R
Vh4	Volt4_R
Vh5	Volt5_R
Vh6	Volt6_R
f_1	1.934e+14
f_2	1.93325e+14
f_3	1.9325e+14
f_4	1.93175e+14
f_c	1.932875000000000e+14
f_out1	Change_fout1
f_out2	Change_fout2
f_out3	Change_fout3
f_out4	Change_fout4

Figure 4.12: Definitions of symbols on OptSim.

2. With OptSim closed, the .moml must be opened with a tex editor and an univocal name is substituted at the variable value in the rows corresponding to each variable. In the same file there cannot be another word equal to the one inserted for each variable; if not, the next step could introduce an error in the simulation.

```
<property name="Vh1" class="ptolemy.data.expr.Parameter" value="Volt1_R">
</property>
<property name="Vh2" class="ptolemy.data.expr.Parameter" value="Volt2_R">
</property>
<property name="Vh3" class="ptolemy.data.expr.Parameter" value="Volt3_R">
</property>
<property name="Vh4" class="ptolemy.data.expr.Parameter" value="Volt4_R">
</property>
<property name="Vh5" class="ptolemy.data.expr.Parameter" value="Volt5_R">
</property>
<property name="Vh6" class="ptolemy.data.expr.Parameter" value="Volt6_R">
</property>
<property name="f_1" class="ptolemy.data.expr.Parameter" value="1.934e+14">
</property>
<property name="f_2" class="ptolemy.data.expr.Parameter" value="1.93325e+14">
</property>
<property name="f_3" class="ptolemy.data.expr.Parameter" value="1.9325e+14">
</property>
<property name="f_4" class="ptolemy.data.expr.Parameter" value="1.93175e+14">
</property>
<property name="f_c" class="ptolemy.data.expr.Parameter" value="1.932875000000000e+14">
</property>
<property name="f_out1" class="ptolemy.data.expr.Parameter" value="Change_fout1">
</property>
<property name="f_out2" class="ptolemy.data.expr.Parameter" value="Change_fout2">
</property>
<property name="f_out3" class="ptolemy.data.expr.Parameter" value="Change_fout3">
</property>
<property name="f_out4" class="ptolemy.data.expr.Parameter" value="Change_fout4">
</property>
```

Figure 4.13: Definition of the new name of the variables in the text editor.

3. The file .moml has to be opened on MatLab and the univocal names, inserted in the variable value, are inverted with the wanted values.

```
fileID=fopen('Benes_64QAM.moml','r');
A=fscanf(fileID,'%c');
newA=strrep(A,'Volt1_R',sprintf('%g',Vh_1));
newA=strrep(newA,'Volt2_R',sprintf('%g',Vh_2));
newA=strrep(newA,'Volt3_R',sprintf('%g',Vh_3));
newA=strrep(newA,'Volt4_R',sprintf('%g',Vh_4));
newA=strrep(newA,'Volt5_R',sprintf('%g',Vh_5));
newA=strrep(newA,'Volt6_R',sprintf('%g',Vh_6));

newA=strrep(newA,'Change_OSNR',sprintf('%g',OSNR_ut));

newA=strrep(newA,'Change_fout1',sprintf('%g',f_out1));
newA=strrep(newA,'Change_fout2',sprintf('%g',f_out2));
newA=strrep(newA,'Change_fout3',sprintf('%g',f_out3));
newA=strrep(newA,'Change_fout4',sprintf('%g',f_out4));
```

Figure 4.14: Subtitution of the variable name of the previous step with the wanted values.

4. The modified file .moml is then saved with a different name from the original one. Creating a new file allows to maintain the changes

done in the steps 1 and 2.

5. Still on MatLab, with a system command the just created .moml file is executed with OptSim.

```
dlmwrite('Benes_64QAM_com.moml',newA,'delimiter','');
Command=sprintf('jetOptSim -runOpf Benes_64QAM_com.moml');
Status(kSim)=system(Command,'-echo');
```

Figure 4.15: Command used to launch the OptSim execution.

6. Once the simulation is finished, the workspace just created from OptSim is loaded and used to calculated the BER; it is obtained through a code that describe the DSP described on MATLAB.

```
load('Benes_WS_1');
     os_RX_DSP
close all
BER_1_final_1_16(iOSNR,1,kSim)=BER;

 load('Benes_WS_2');
    os_RX_DSP
close all
BER_2_final_1_16(iOSNR,2,kSim)=BER;

 load('Benes_WS_3');
    os_RX_DSP
close all
BER_3_final_1_16(iOSNR,3,kSim)=BER;

 load('Benes_WS_4');
    os_RX_DSP
close all
BER_4_final_1_16(iOSNR,4,kSim)=BER;
```

Figure 4.16: Code used to calculate the Bit Error Rate for each workspace.

In this case there are four different receivers so four different workspaces are created; for each of them the BER is calculated and saved in a different variable.

This procedure (except for the first two points) is repeated for each iteration. In this way it is possible to change each variable and to assign to it the wanted value.
The values of the six voltages and the resonance frequencies are taken from the table created from the function "Perm func" as is shown in the following figure.

```
M_f=Perm_func(3, 2);
CH=[f_2 f_3 f_4 f_1];
f_out1=CH(M_f(kSim,8));
f_out2=CH(M_f(kSim,9));
f_out3=CH(M_f(kSim,10));
f_out4=CH(M_f(kSim,11));


Vh_1=Vc*M_f(kSim,2);
Vh_2=Vc*M_f(kSim,3);
Vh_3=Vc*M_f(kSim,4);
Vh_4=Vc*M_f(kSim,5);
Vh_5=Vc*M_f(kSim,6);
Vh_6=Vc*M_f(kSim,7);
```

Figure 4.17: Assignment of the values for each iteration.

The two inputs inserted in the "Perm func" are respectively the number of rings in the rows and in the columns of the used Benes; in this case there are three rings horizontally and two vertically. The entire matrix described above and generated by the function is saved in the variable M_f.
CH is a vector in which are saved the four central frequencies and it is used to assign the output frequency at the variable $f_out_{1,2,3,4}$ that are substituted in the moml file.. In this way the last four columns of the matrix M_f are used to select the position of the vector CH.
Regarding the six voltages, it is simpler because in the table there is 1 where it needs an high voltages and a 0 where it needs low voltage; its enough multiply the corresponding value of M_f with the voltage value (Vc).

4.4.4 | Description of the simulation campaign

In this section all simulations done are described in order to cover all aspects of the device.
The frequency responses of the switches are reported in the section 4.3, the behaviour of the Benes Switch is described with the Transmitter.

Figure 4.18: OptSim screenshot with one Transmitter and a coherent Receiver.

One by one, all four input ports have been connected to the Transmitter in order to verify the symmetry of the Switch; each time the input changes, the BER is calculated, in order to be sure that the behaviour is the same.
As expected, the result is the same between the four ports and this is due to the fact that whatever is the input port, the signal passes through the same number of rings.
In order to show if the Raised Cosine in input is filtered or distorted,the figure below shows the comparison between the input and output signals of a Benes Switch composed by the Double Rings.

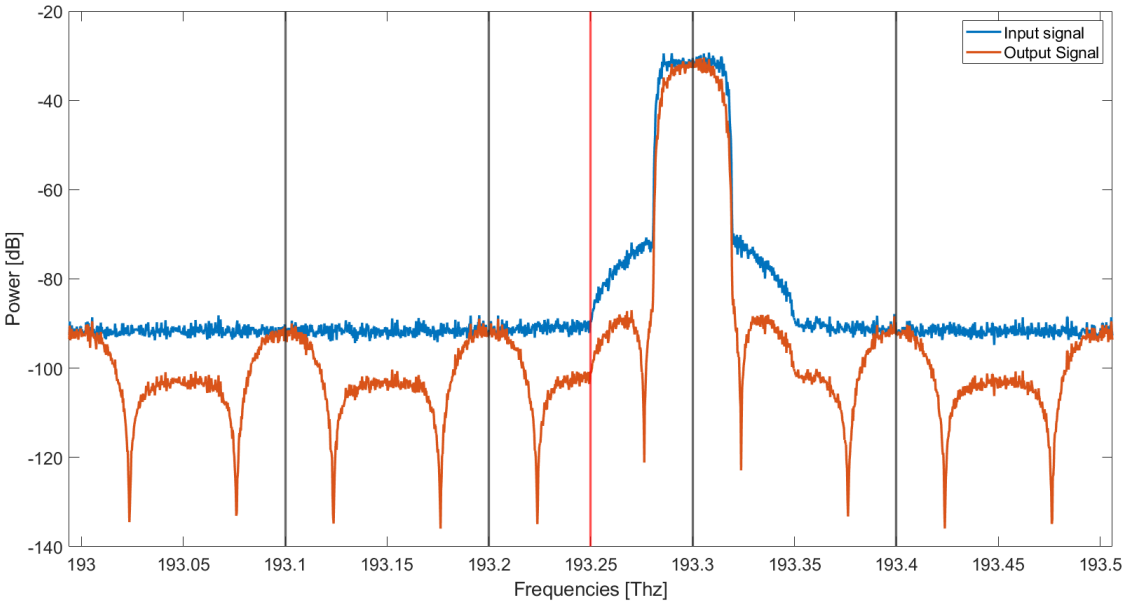

Figure 4.19: Comparison between the input signal and the output signal (second order Ring): Case 1.

In the case showed in figure 4.19 the input is in the port 2 of the switch so the output can be found in the port 4 because, the curve above has been generated with all voltages of the rings equal to $0V$.
In the same conditions, also the Benes composed by six first order rings has been simulated; the figure 4.20 switches the comparison between input and output.

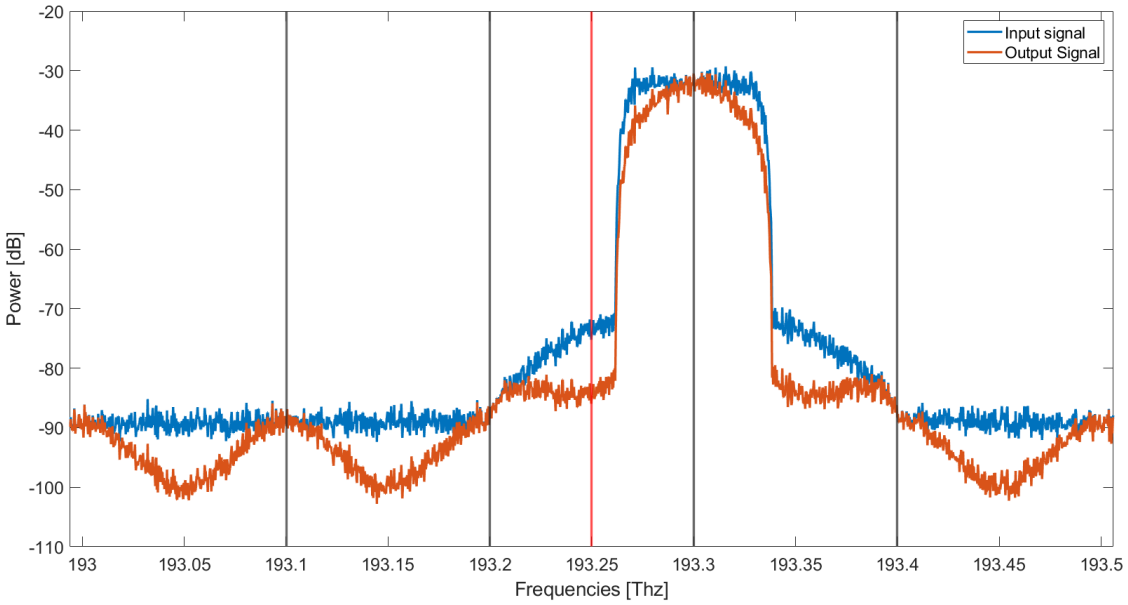

Figure 4.20: Comparison between the input signal and the output signal (first order Ring): Case 1.

From the two plots it can be seen that in the case with the larger bandwidth, the filtering effect is stronger with respect to the one with the narrower bandwidth. This is an expected outcome because, even if the single ring has a larger band with respect to the double one, it is not enough wide to make the whole signal passes entirely but it is slightly filtered.

Another combination of voltages is described below; the case number 3 has been chosen with the voltage in the ring 5 equal to $V_{h5} = 8.4V$. In this case the output sequence is: [1 4 3 2].
For this example the input port 3 is fed by the transmitter with a signal centered at the frequency f_3 and the receiver is connected to the output port 3.
As in the previous example, the comparisons between the input curve and the output curve in the two cases are shown below.

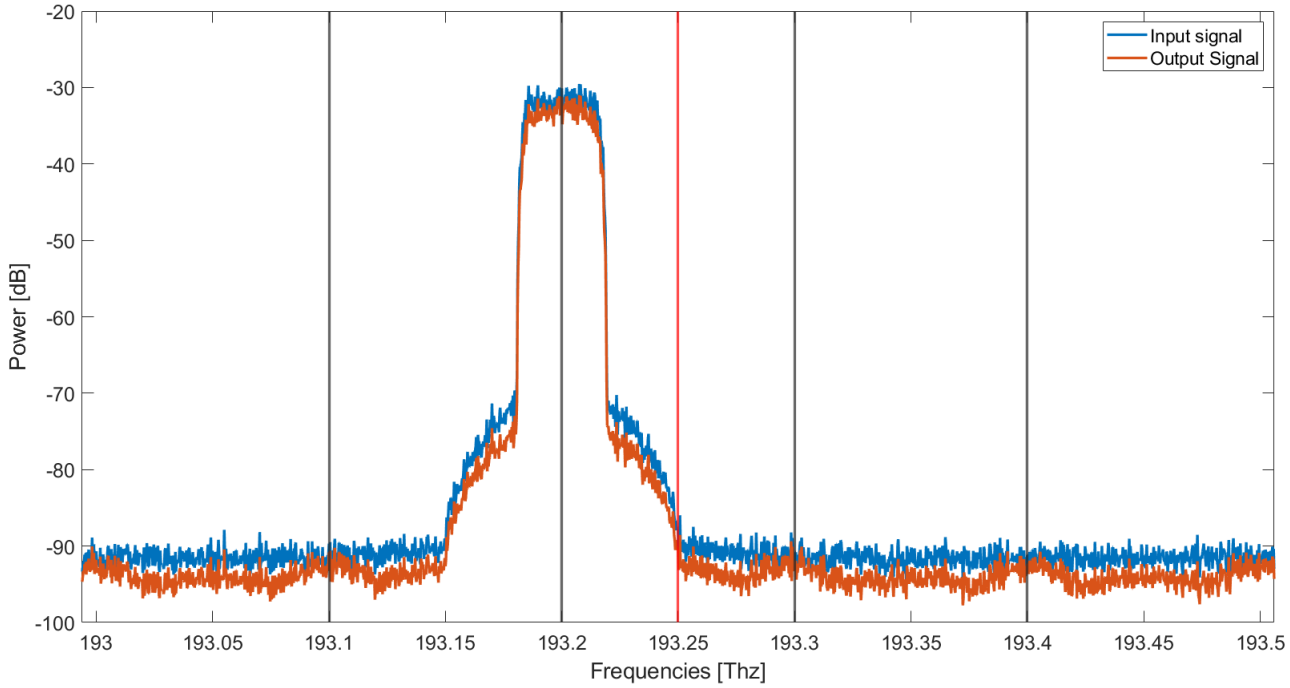

Figure 4.21: Comparison between the input signal and the output signal (second order Benes): Case 3.

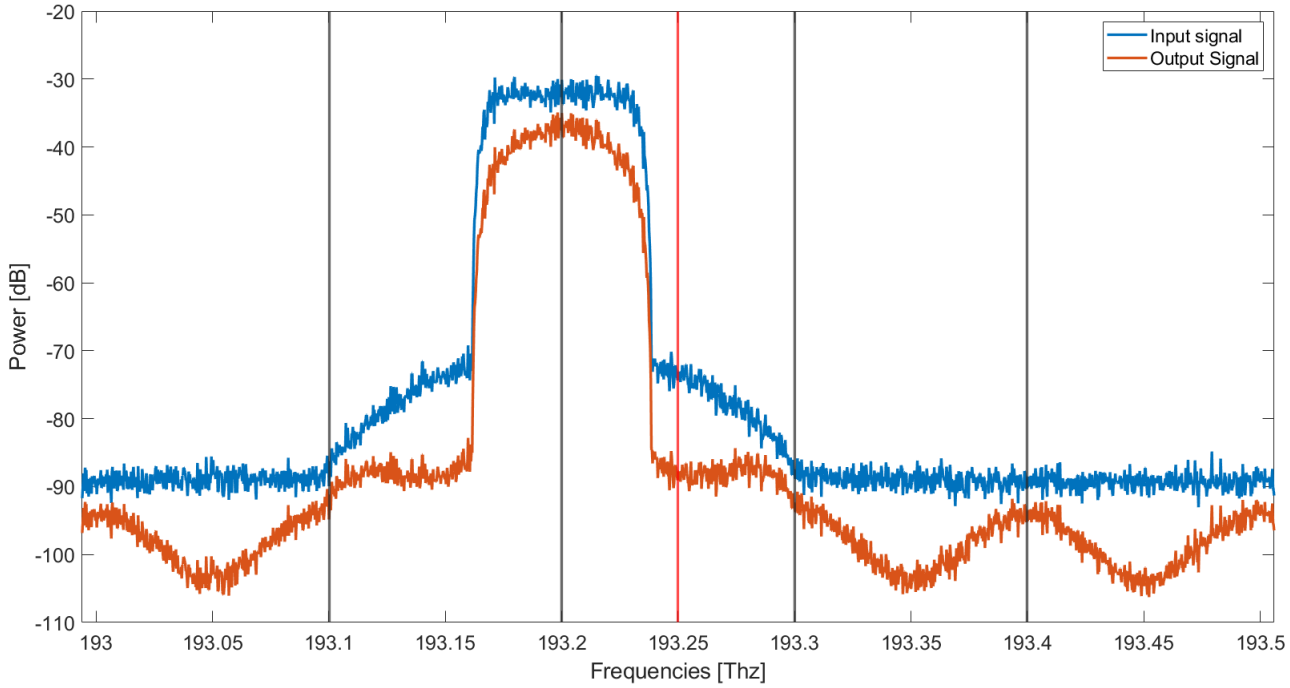

Figure 4.22: Comparison between the input signal and the output signal (first order Benes): Case 3.

Regarding the double ring, the difference with respect to the case 1 is minimal: a slight attenuation can be noticed but at the same time the filtering effect is less important so, in terms of BER, the two cases are very similar.
Looking at the signal with the larger bandwidth in output of Benes Switch with the ring of the first order, the power attenuation is dominant in this case. For this reason, in the Benes of the first order, the results reported in the following chapter have been obtained with the block for the filtering and power normalization of the signal.

In the next step, all input ports are fed by four transmitters and in output there are four receivers; each of them calculates the BER in a specific channel.
For the next simulations and results, the input sequence chosen is the following: $[f_1\ f_2\ f_3\ f_4]$. This means that the transmitter connected to the port 1 generates a signal centered at f_1 up to the transmitter on the port 4 that generates at f_4. The figures 4.23 and 4.24 shows the input signals used respectively for the Benes Switches composed by the first and the second order Rings.

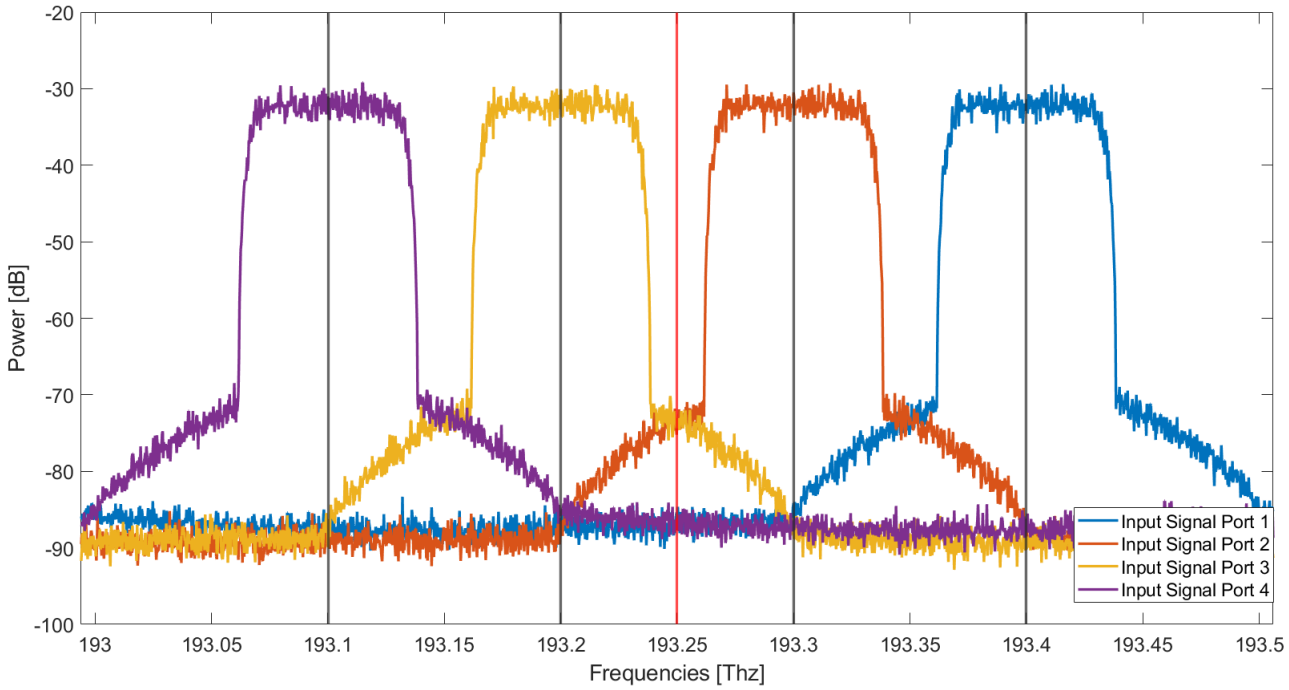

Figure 4.23: Input signals generated from 4 Transmitters centered at the four working channels.

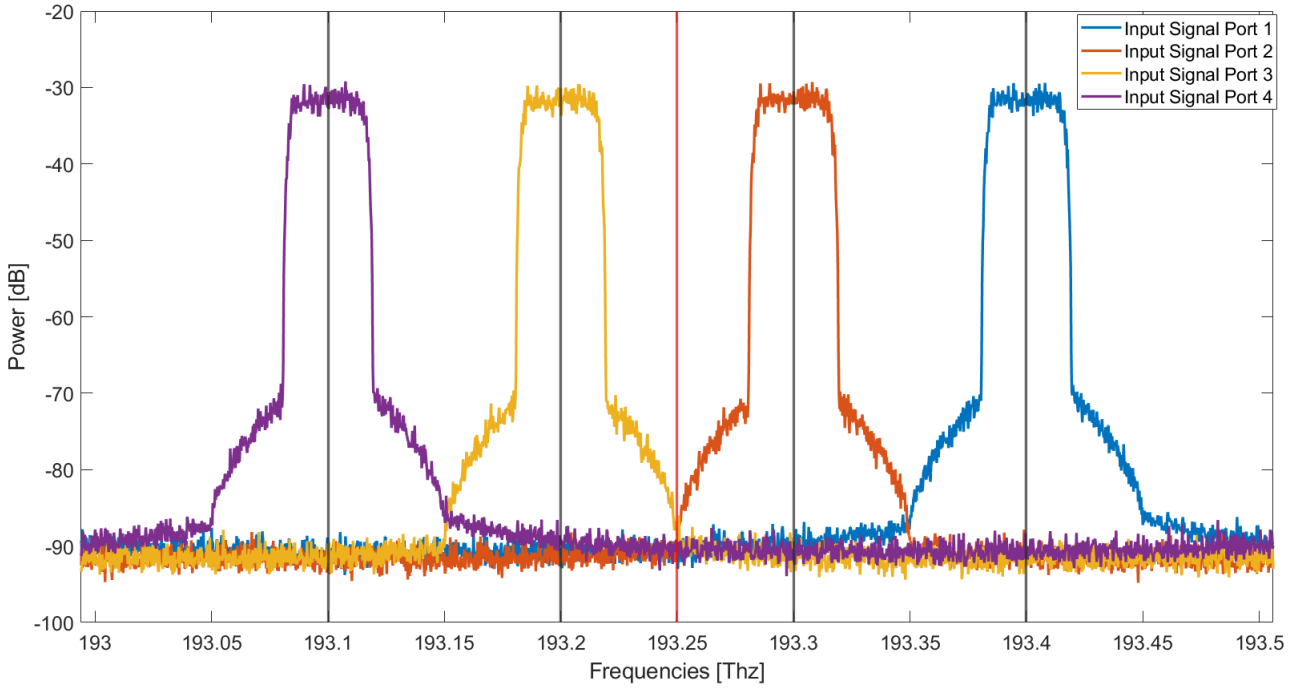

Figure 4.24: Input signals generated from 4 Transmitters centered at the four working channels.

From the figure above can be seen that the four signals are not overlapped and this means that there should be no difference, in terms of BER, between when there is one input and when there are four. This will be confirmed in the next chapter when the curves of BER will be reported.
In order to show the filtering and attenuation effects, the figure below displays the four output signals compared with the corresponding input signals in the 'all-zero voltage' configuration.

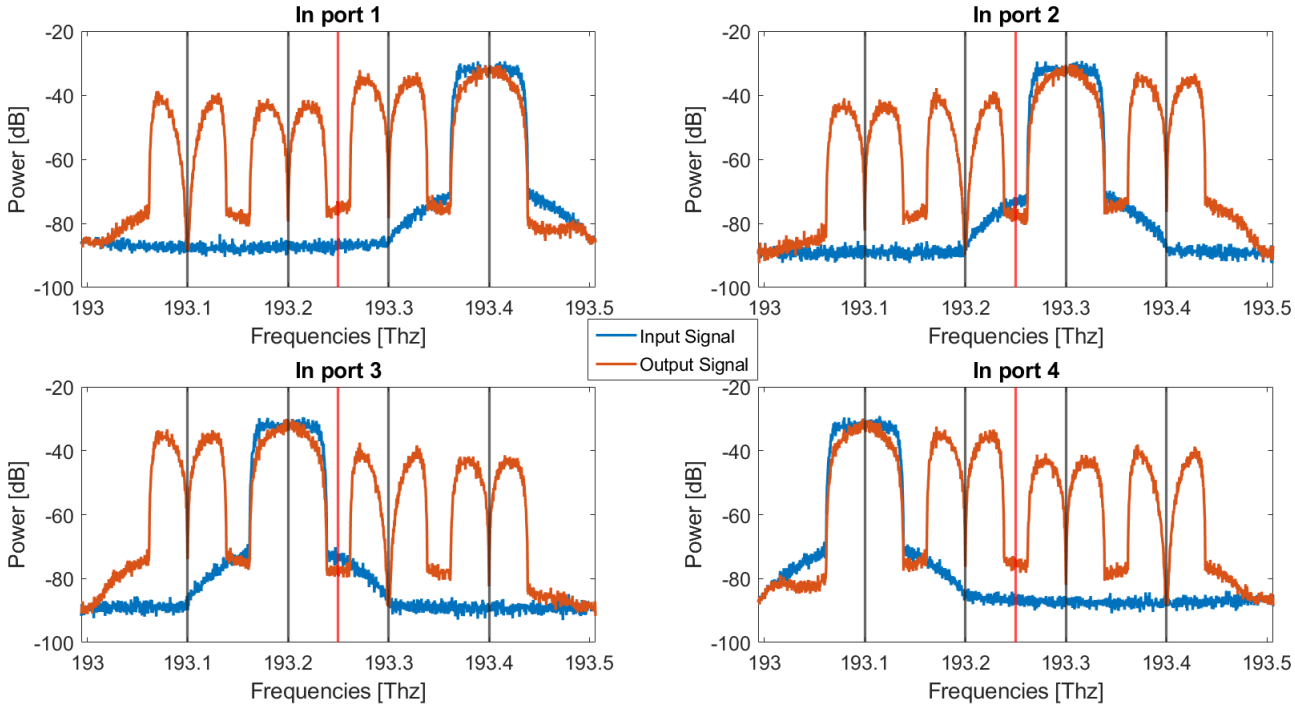

Figure 4.25: Subplot 2x2 of the output of the Benes with the first order Rings: Case 1.

The curves have been coupled as follows:

- Graph (1,1): Input 1⇔Output 3.
- Graph (1,2): Input 2⇔Output 4.
- Graph (2,1): Input 3⇔Output 1.
- Graph (2,1): Input 4⇔Output 2.

This is the output order that corresponds the the first case in the table shown in figure 3.10.
From the 2x2 subplot can be seen that all four signals are filtered and attenuated in the same way. The most important aspect is that in this case the signals are filtered in the same way as the case of the single transmitter; this is fundamental because means that all ports of the switch can be used simultaneously without an additional penalty. This does not guarantee that for each voltage combination, the BER curves of the four ports will be equals each other. Changing the six voltages, the four signals have different paths so the effects of the rings are different on the four spectra. The figure 4.26 shows the output Spectra of the Benes of the second order in the same conditions of the previous one.

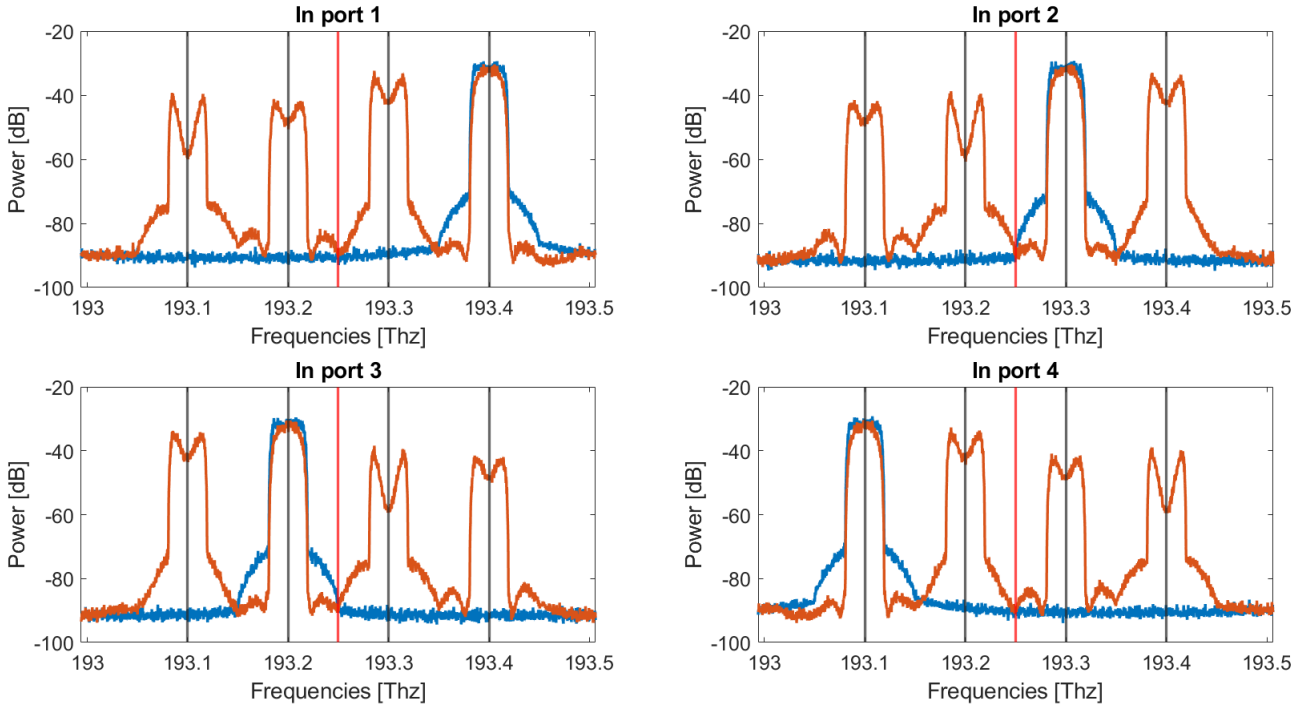

Figure 4.26: Subplot 2x2 of the output of the Benes with the second order Rings: Case 1.

The most important features are the same of the previous one so, all signals are filtered in same way and, mostly, they are filtered as the case with one input. Also with this type of device, all inputs can be stimulated at the same time.

As for the single input case, the combination 7 of voltages has been analyzed with the following values: $V_{h1} = 0V$,$V_{h2} = 0V$,$V_{h3} = 0V$,$V_{h4} = 8.4V$,$V_{h5} = 8.4V$,$V_{h6} = 0V$. The output sequence is [1 3 4 2] so the input 1 is expected to be found in port 1, the input 2 in the port 3 and so on. The figures 4.27 and 4.28 show the 2x2 subplots of the results of the case 7 with four input signals.
The curves have been coupled as follows:

- Graph (1,1): Input 1⇔Output 1.
- Graph (1,2): Input 2⇔Output 4.
- Graph (2,1): Input 3⇔Output 2.
- Graph (2,1): Input 4⇔Output 3.

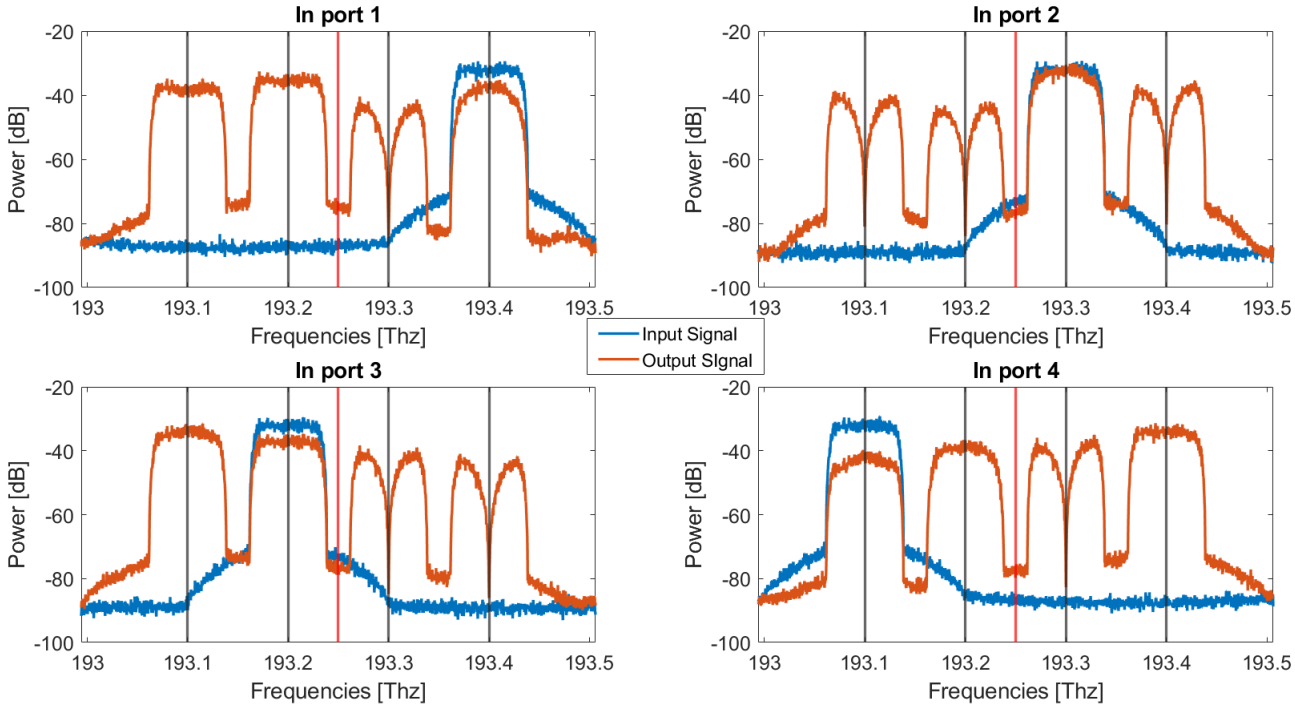

Figure 4.27: Subplot 2x2 of the output of the Benes with the first order Rings: Case 7.

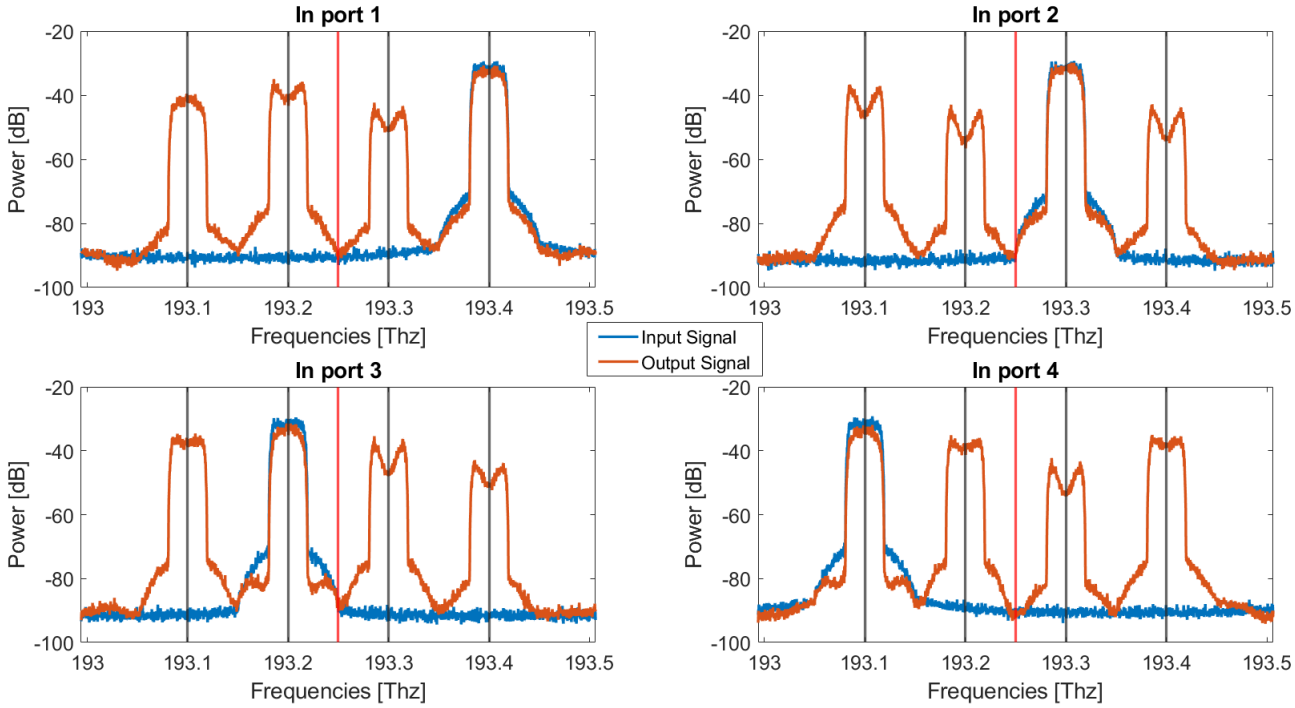

Figure 4.28: Subplot 2x2 of the output of the Benes with the second order Rings: Case 7.

As for the previous case, in the Benes with the first order ring, the power attenuation effect is more present with respect to the second order. With first order Ring, the output signal has a power level lower than the input signal; this is due to the attenuation of the through port of the single ring. In the channels where is more attenuated with respect to the others, the signals crosses the thought port more than one time.
In the case with the Second order Rings, there is not power attenuation but the difference between two outputs can be only in the filtering effects. These last depends on the path that the signal must run across the six rings in the switch.

5 Simulation Results

In this Chapter, the results in terms of BER are reported and described. The study as been done choosing a BER target and finding for each iteration which is the OSNR necessary to reach that value. In this work the BER target is equal to $1.7 * 10^{-2}$.
In addition, also the OSNR in the target with the TX and the RX directly connected has been founded; this value is subtracted to the previous ones with the device, in order to calculate the penalty ([dB]) due to the Switch. The bit error rate (BER) is the number of bit errors divided by the total number of transferred bits in a time interval.

5.1 | Results: Second Order Ring

In order to report the results of the study of this thesis, all 64 cases of voltage combinations have been simulated; for each of them, the OSNR has been changed from 16 dB to 25 dB.
The OSNR has been changed in order to find the value in which the $BER = 1.7 * 10^{-2}$.
With a post processing work, using the interpolation function, from each of the 64 levels, four values has been obtained passing to a two dimension matrix. The obtained values are the OSNR necessary to reach $BER = 1.7 * 10^{-2}$. Finally, to each term, the OSNR necessary to reach the target without Benes Switch between TX and RX has been subtracted. The final matrix contains the penalty [dB] introduced from the device, for each of the 64 combinations in the four output ports.
The possible output sequences are $4! = 4 * 3 * 2 = 24$ but there are 64 voltage combinations; different voltage combinations produce the same output sequence.
This device has been designed and analyzed with the purpose to address the input information in any of the four output ports; for this reason in the results below, the best case of each output sequence is reported. The best case is the one with the lower maximum among the four ports.
The figure 5.1 shows the table of the 24 best cases simulating the Benes Switch composed by six second order Rings.
Over the 64 cases, if there are two of them that have the same output order, the one with the lower maximum is considered the best one for

that particular output order.

Output Sequence	Cases	Penalty Port 1	Penalty Port 2	Penalty Port 3	Penalty Port 4
1234	19	3.4880	3.3709	3.4006	3.4555
1243	20	3.4880	3.3709	1.4227	1.3301
1324	8	1.7286	2.8547	2.8430	2.5636
1342	58	2.6928	2.8743	3.3755	1.5714
1423	61	2.6939	1.7394	2.8422	3.3290
1432	3	1.7261	1.1298	1.6962	0.9887
2134	27	1.4139	1.4814	3.4006	3.4555
2143	52	1.3993	1.4773	1.4319	1.3482
2314	40	3.3493	2.8536	1.6385	2.5788
2341	39	3.3493	2.8536	3.3724	2.8939
2413	36	3.3460	1.0324	1.6165	3.3317
2431	35	3.3460	1.0324	1.6972	2.8955
3124	49	0.9689	3.4736	2.8345	1.7052
3142	50	0.9689	3.4736	3.3755	1.5714
3214	17	0.9741	1.6640	0.8410	1.7094
3241	47	1.6096	2.7643	3.3724	2.8939
3412	1	2.8970	2.8859	2.8652	2.9727
3421	2	2.8970	2.8859	0.7378	0.7144
4123	53	2.9301	3.4637	2.8422	3.3290
4132	54	2.9328	3.4624	2.6865	1.5627
4213	21	2.9273	1.6719	0.8563	3.3238
4231	22	2.9273	1.6719	2.7092	2.8817
4312	9	0.4003	0.7650	2.8652	2.9727
4321	6	0.3207	0.5287	0.6761	0.5980

Figure 5.1: Table of the best cases.

In the first column there are the 24 output sequences in ascending order. The second column indicates for each sequence, the case with the best behaviour, among the 64 combinations while the others are discarded.
The last four columns represents the penalty of the four ports for each combination.

In order to shown the behaviour of the 24 Cases described above, the following four graphs show the BER in function of the OSNR at which they have been simulated.

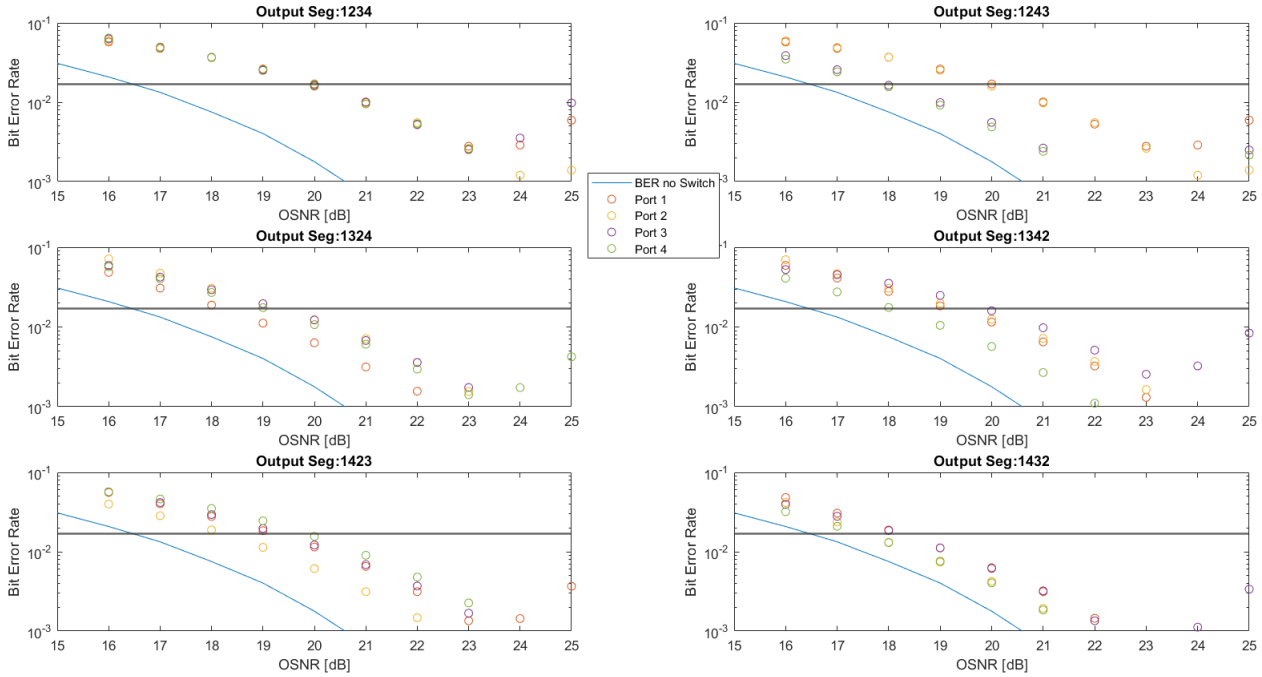

Figure 5.2: Subplot 3x2 of the BER with sequences 1234, 1243, 1324, 1342, 1423, 1432.

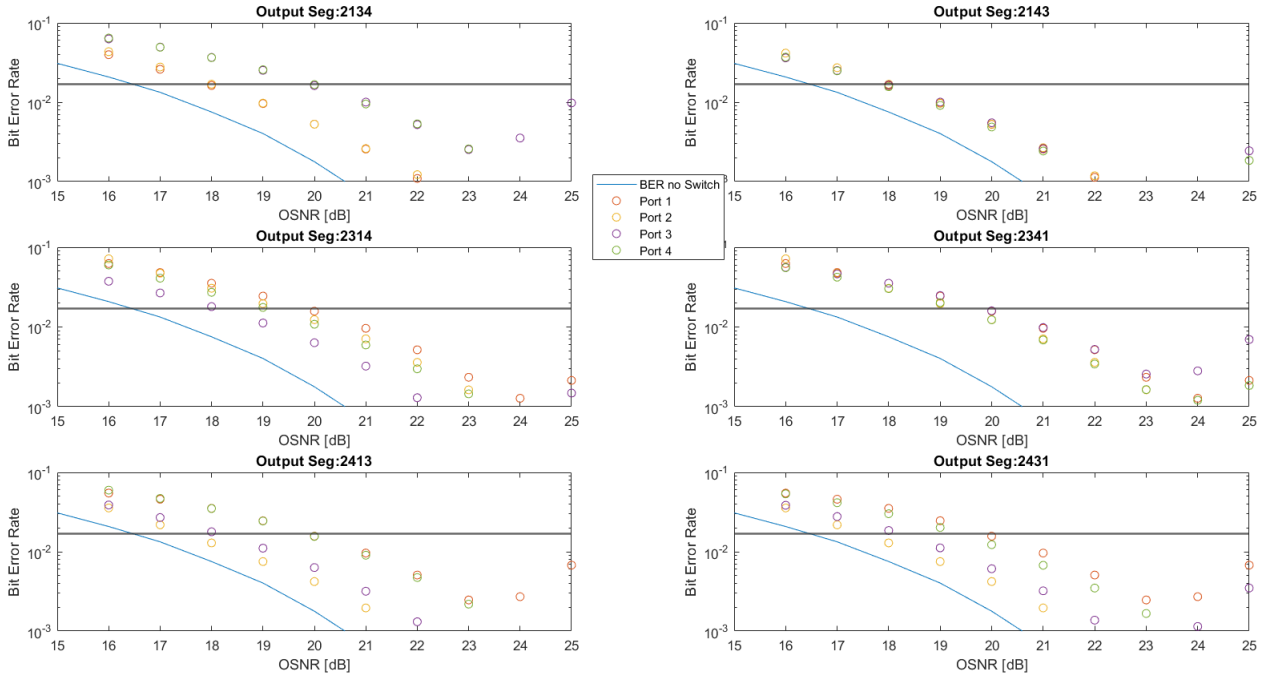

Figure 5.3: Subplot 3x2 of the BER with sequences 2134, 2143, 2314, 2341, 2413, 2431.

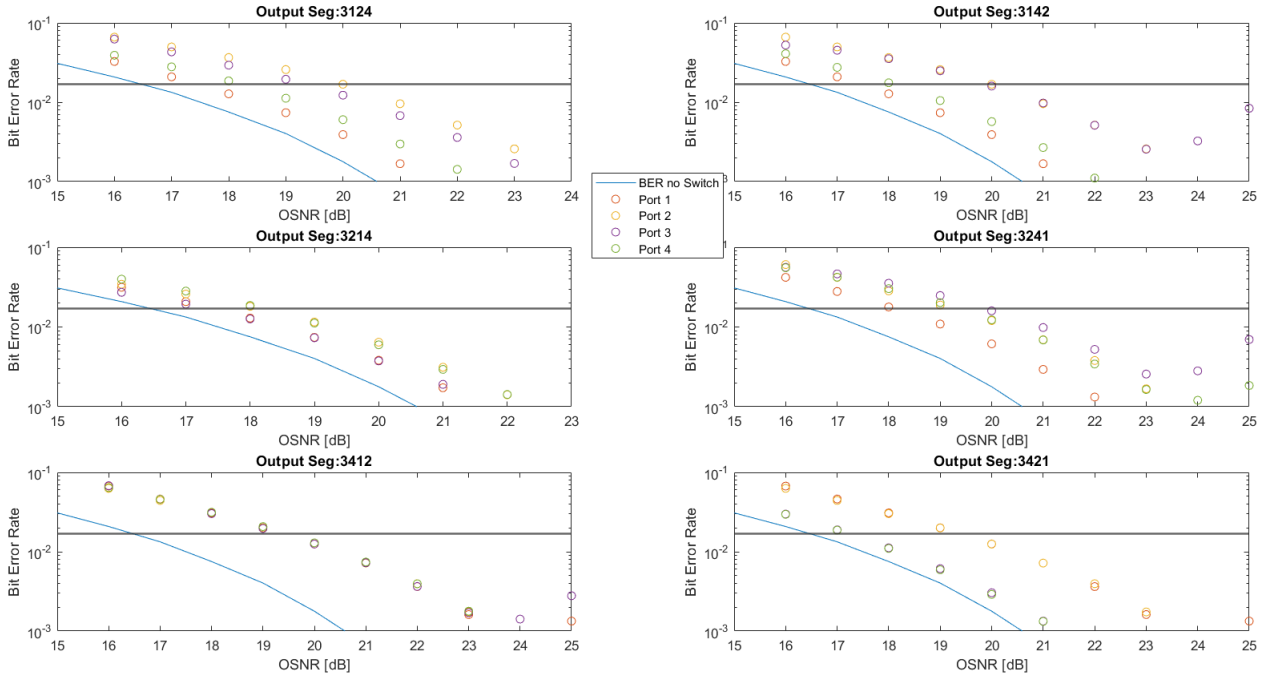

Figure 5.4: Subplot 3x2 of the BER with sequences 3124, 3142, 3214, 3241, 3412, 3421.

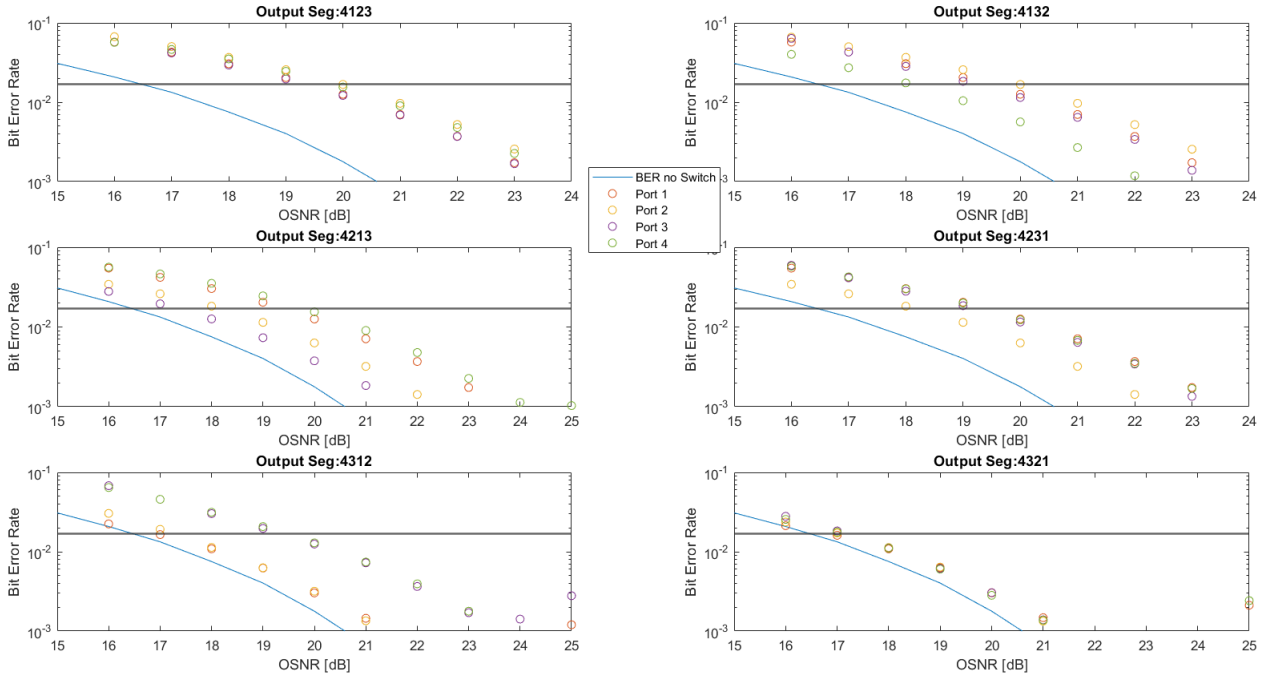

Figure 5.5: Subplot 3x2 of the BER with sequences 4123, 4132, 4213, 4231, 4312, 4321.

In the graphs, in the ordinates there is the OSNR vector simulated on OptSim for each combination; in the abscissa there is the $log_{10}(BER)$ calculated.
The blue curve is the BER obtained connecting directly the Transmitter and the Receiver back-to-back; this curve is used as a reference to see the impact of the Benes in the quality of the transmission. The horizontal black line represents the BER target at $1.7 * 10^{-2}$. Finally the dots of different colors are the BER values calculated with the Benes; each color corresponds to a Port in the corresponding combination.
Obviously they are all different because for each graph, the voltages on the six rings are combined in different way so the path that the signal must cross is different.
The maximum penalty is about 3.5 dB while the minimum value is less than 1 dB; the mean value above the 24 shown is 2dB. This can be see more easily in the figure 5.6.

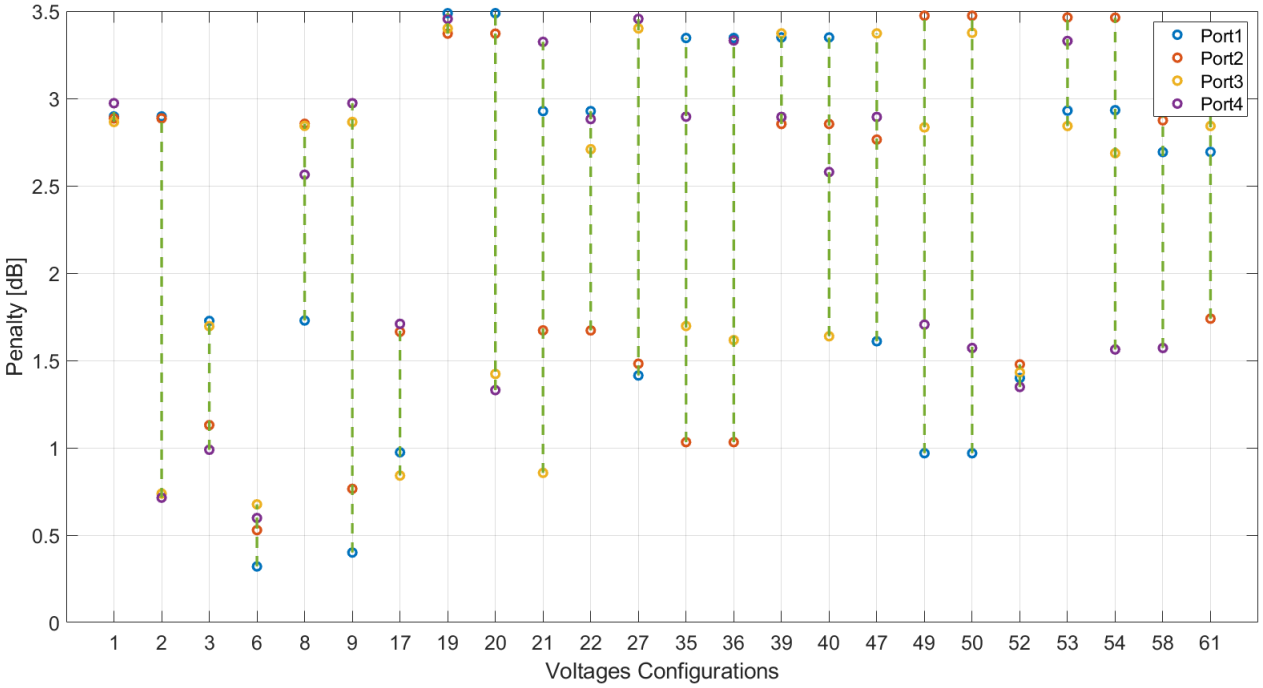

Figure 5.6: Penalty of the four ports in the 24 best cases.

In the ordinates there are the 24 best cases while in the abscissa there is the penalty [dB]. In the x axis, just the cases reported in the table in figure 5.1 are shown.
Also in this case the four colors corresponds to the four ports and they represent the behaviour of the penalty in the cases.

5.2 | Results: First Order Ring

Regarding the Benes Switch with the first order rings, the result are reported in the same mode of the previous section. Also in this case, over the 64 voltage configurations, 24 have been selected. For every different output order, the best case has been chosen taking into account the minimum maximum of the four ports.
In this case the Benes Switch has been simulated with the Power normalization blocks connected between the outputs of the device and the input of the receivers.
The following four figures shows the BER curves of the four ports of the 24 Best cases.

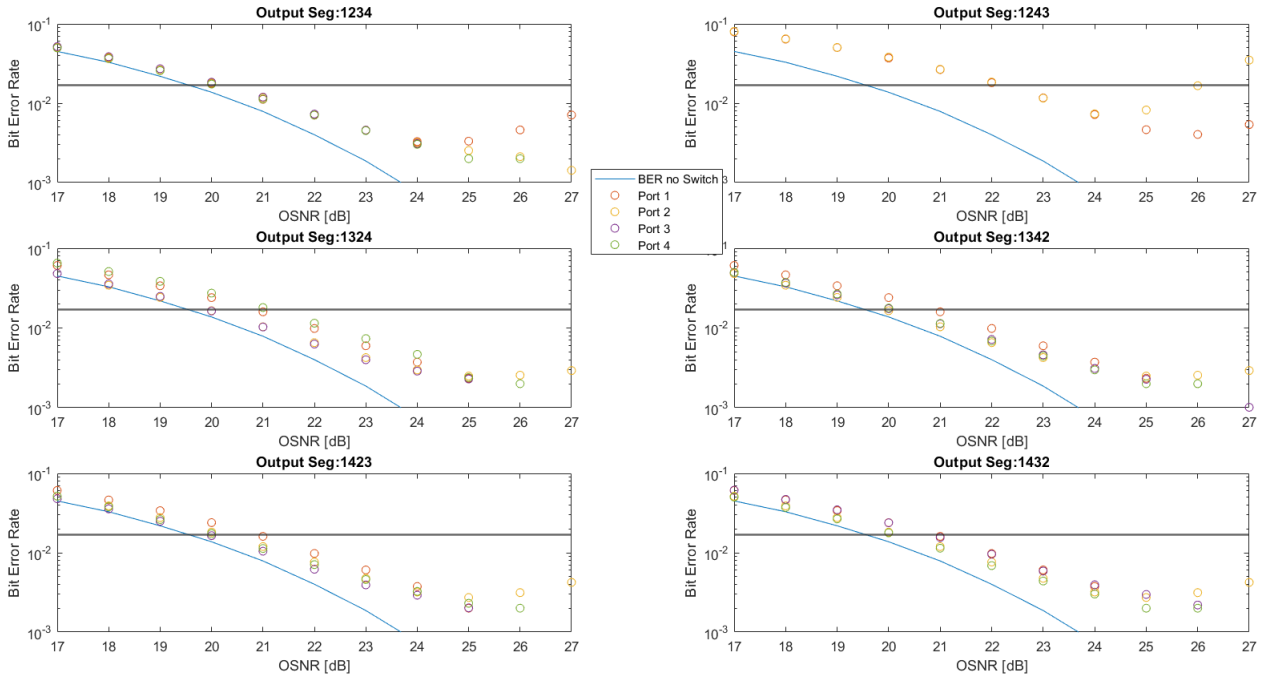

Figure 5.7: Subplot 3x2 of the BER with sequences 1234, 1243, 1324, 1342, 1423, 1432.

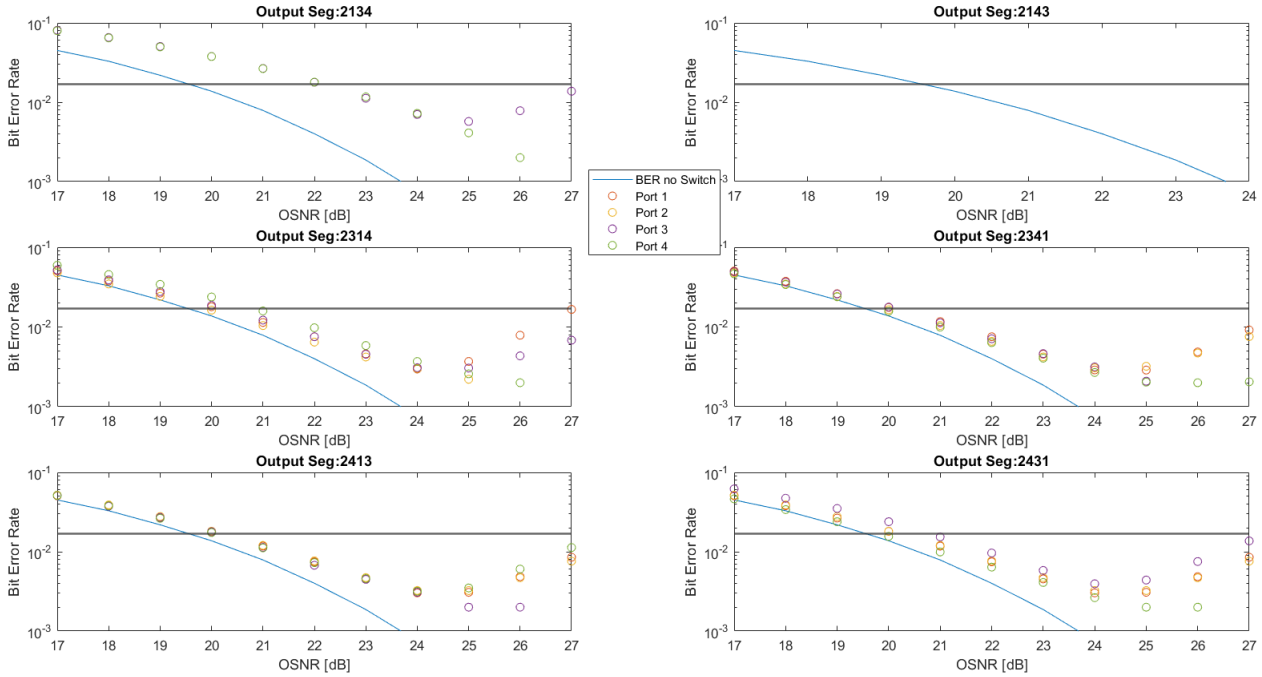

Figure 5.8: Subplot 3x2 of the BER with sequences 2134, 2143, 2314, 2341, 2413, 2431.

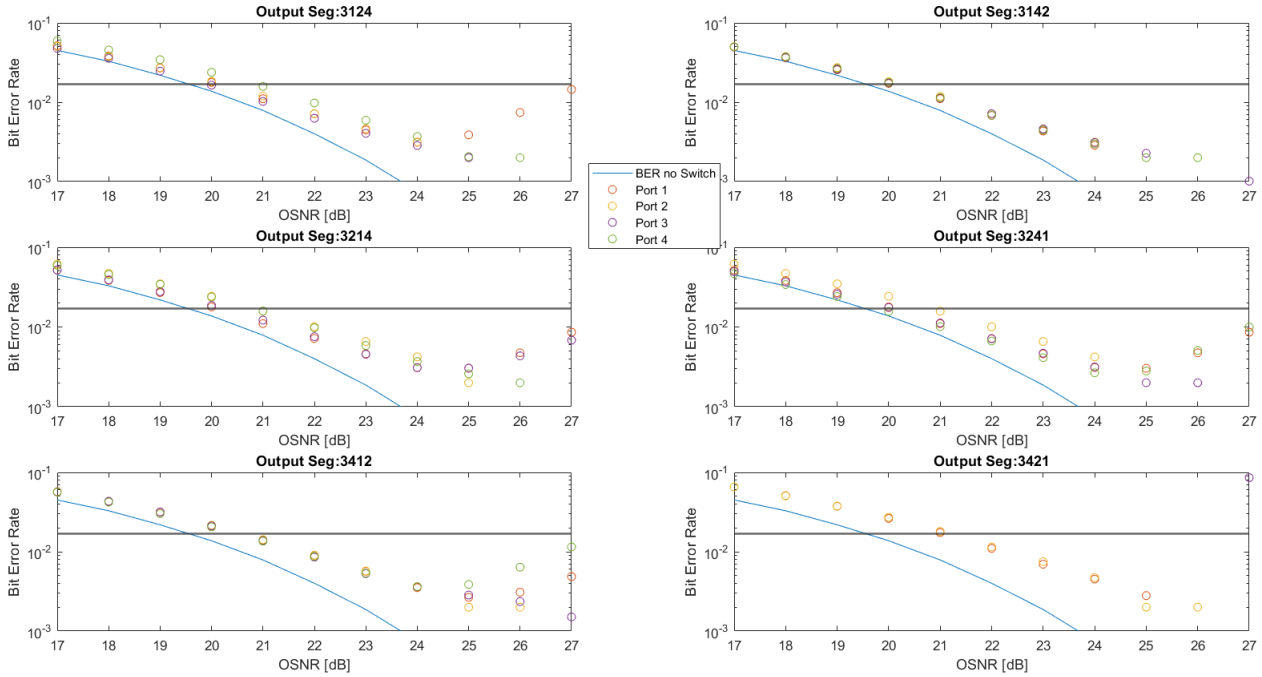

Figure 5.9: Subplot 3x2 of the BER with sequences 3124, 3142, 3214, 3241, 3412, 3421.

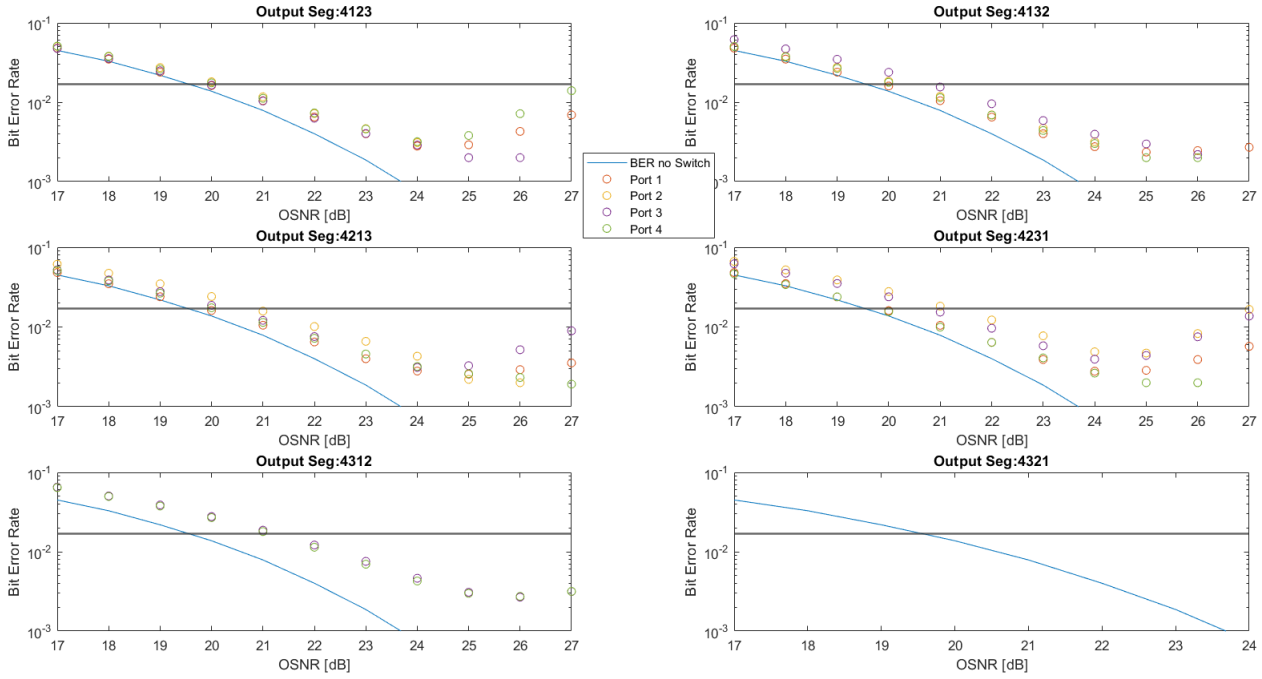

Figure 5.10: Subplot 3x2 of the BER with sequences 4123, 4132, 4213, 4231, 4312, 4321.

The mean value of the Penalty in this case is about 1.5 dB. With this results the power attenuation effects are not taken into account but just the filtering effects.
With respect to the case with the Double rings, the Benes Switch composed by the rings of the first order does not work properly for all cases. In two graph of the previous figures, two curves are not showed because they have a penalty too high to be seen. This means that the output orders 2143 and 4321 can not be used with this device.
This is due to the path that the signal must follow inside the Benes Switch; some voltage combinations cause an interference that distorts the signal information. The figure 5.11 shows the penalty of the 24 selected cases.

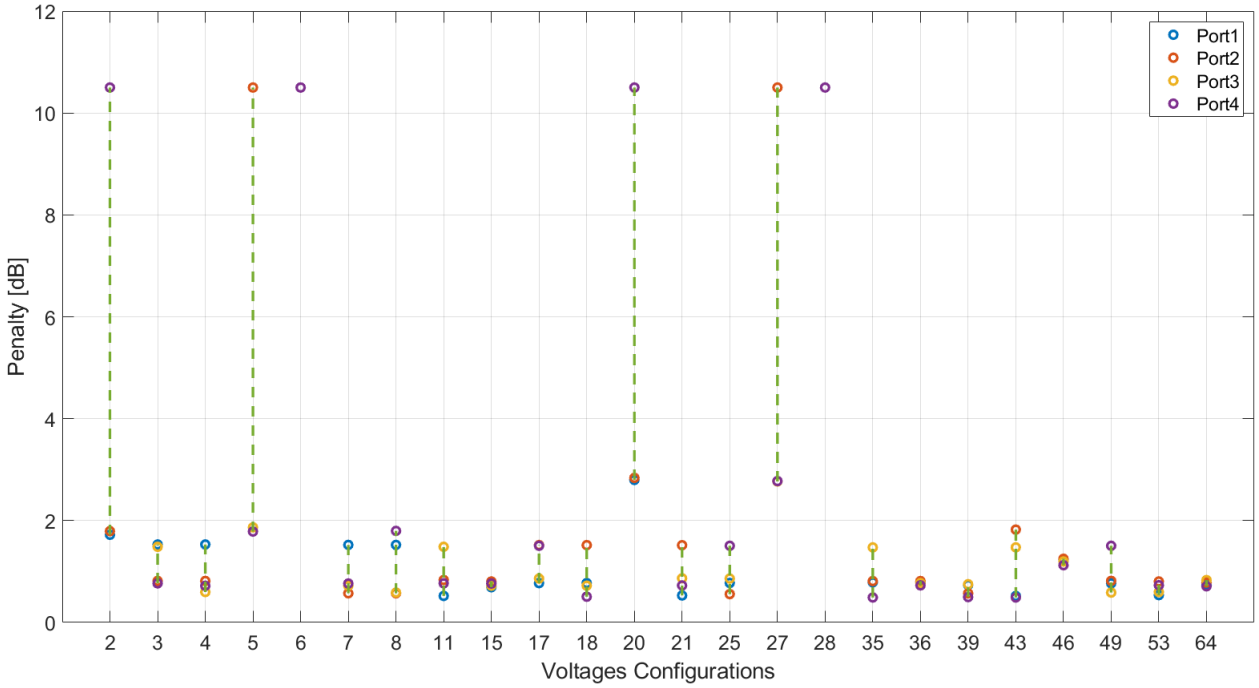

Figure 5.11: Penalty of the four ports in the 24 best cases.

Here is more clear how some combinations does not have good performances in terms of BER. The mean value of the penalty in the other cases is lower then the previous case; the filtering effect are not so evident. Anyway, in the applications with the input signals at 64 GBaud, this device cannot be fully employed because not all output permutations can be found in output. This is a perfect starting point for a future implementation with different kind of elements that can substitute the actual.

6 Conclusions

The purpose of this thesis was to design and simulate a Switch with a Benes structure with four input ports and four output ports.
The main function that the device should have is to direct input signals from one input port to any of the output ports at one of the working frequencies.
The starting point was the design of the single element that composes the switch.
In this work, a micro ring filter was chosen because, with this component, applying a voltage to the heating port, it is possible to shift its frequency response. The shift in frequency is proportional to the absolute values of the voltage applied; this means that a negative or positive potential have the same effect.
Two types of micro-ring were designed and simulated: a first order Ring, composed by two waveguides and one loop between them, and a second order Ring, composed of two loops between the two waveguides.
Theoretically the first one should have a larger bandwidth in one port, but a strong attenuation in the other. The second one should have, in the two output ports, two more similar frequency responses; the consequence is a narrower bandwidth in one port but almost no attenuation in the other.
The analyzed band was 500 GHz and it was divided in 4 channels, distant 100 GHz from each other. The Rings were designed in order to have a frequency response resonant at one of the working frequencies (the central frequency of each channel) and with a FSR (Free Spectral Range) of 100 GHz. To achieve this goal the length, the coupling coefficients and the refractive index were found and inserted in the OptSim tool in order to simulate the device.
After the design, six rings were connected to construct a Benes structure, with four inputs and four outputs.
The signals sent to the Benes were PM-64QAM centered at one of the four wavelengths and generated by four transmitters. In frequency domain, the signal has a raised cosine shape with $\rho = 0.2$. To calculate the Bit Error Rate (BER), four coherent receivers were connected to the outputs of the Benes, each one centered in the proper channel.
The characterization of the device was made integrating the tools MAT-

LAB and OptSim.
In the final simulations, the OSNR for each combination of voltages was changed from 18 dB to 25 dB. The results obtained confirm that the Benes Switch analyzed can direct the power of an input signal centered at one of the working frequencies to any of the output ports.
This result could lead to a bigger application, where the Switch is used as a single element to construct a Benes structure of higher level. In this way a switch that can manage dozens of channels can be obtained.
A possible improvement is to substitute the single element that composes the switch with a third order ring in order to have a frequency response with steeper edges. Another solution could be to use a ring composed by two loops and two waveguides like the one used in this thesis, but with a different layout: two crossing waveguides both coupled with the two loops.
The most important achievement of this thesis is the creation of a simulations framework of a silicon photonics device that start from the Mask level up to the system level.

Bibliography

[1] Sotirios Papaioannou, K. Vyrsokinos, O. Tsilipakos, A. Pitilakis, K. Hassan, J.-C. Weeber, L. Markey, A. Dereux, S. I. Bozhevolnyi, A. Miliou, E. E. Kriezis, and N. Pleros
A 320 Gb/s-Throughput Capable 2 2 Silicon-Plasmonic Router Architecture for Optical Interconnects, JOURNAL OF LIGHTWAVE TECHNOLOGY, VOL. 29, NO. 21, NOVEMBER 1, 2011

[2] Dessislava Nikolova, Sébastien Rumley, David Calhoun, Qi Li, Robert Hendry,Payman Samadi, and Keren Bergman
Scaling silicon photonic switch fabrics for data center interconnection networks., OPTICS EXPRESS 1159, 20 Jan 2015

[3] Qi Li, Dessislava Nikolova, David M. Calhoun, Yang Liu, Ran Ding, Tom Baehr-Jones,Michael Hochberg, and Keren Bergman
Single Microring-Based 2 × 2 Silicon Photonic Crossbar Switches., EEE PHOTONICS TECHNOLOGY LETTERS, VOL. 27, NO. 18, SEPTEMBER 15, 2015

[4] Lukas Chrostowski. Michael Hochberg
Silicon Photonics Design.